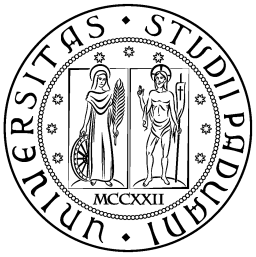

UNIVERSITÁ DEGLI STUDI DI PADOVA

DIPARTIMENTO DI INGEGNERIA INDUSTRIALE

Corso di Laurea Magistrale in Ingegneria Chimica e dei Processi Industriali

Experimental Study on Shear-Induced Percolation in Particle Beds of Granular Materials

Studio sperimentale della percolazione in letti sottoposti a shear

Studente:
Pietro Rando

Relatore:
Prof. C. Andrea Santomaso
Co-Relatore:
Dott.ssa Silvia Volpato

A.A. 2016/17
2 Dicembre 2017

Contents

List of Figures

List of Tables

Introduction

The purpose of this work is to examine the behavior of granular mixtures under controlled conditions. Mixtures of powders are naturally characterized by the tendency to segregate because of different mechanisms. One of these mechanism is called percolation; it is the movement of the small particles of a mixture through the voids between the coarser ones. The percolation velocity and the diffusion of the fine particles through a bed of coarser ones have been studied through an experimental approach using a simple shear box which permits to induce and control the desired shear rate to study this phenomenon; furthermore the effect of the shear rate on the percolation speed has been investigated in different beds made of spherical and irregular particles.

Granular materials are frequenlty used in the industries such as pharmaceutical, food, minerals, fertilizer, energy production and many others. While there have been performed a lot of reaserches on the fluids, this subject has been "underconsidered" for many years; but in the last years it is having great interest. It is important to understand the causes and the behavior of parameters which are crucial in percolation, to optimize the quality product required.

Almost of the authors have studied percolation using a simulation approach: FEM (Finite Element Methods), DEM (Discret Element Methods) and MonteCarlo Analysis. In the literature, there are only few experimental studies on percolation. The first and most important was made by Bridgwater, who developed a simple shear box to study the behavior of the glass spheres percolation; from his articles, it is possible to see which are the most relevant parameters which influence the percolation rate, such as the difference of the sizes of particles and their densities difference.

A problem that the authors have not considered is that the behavior and the shape of the glass spheres is too ideal; the friction coefficient is very small; furthermore the spheres shape can be taken only as a reference. Indeed powders and granular materials are charaterized by a typical shape which is intrinsic to every material.

So it is possible to conclude that to perform experiment using glass spheres can be useful to understand the importance of the different parameters which influence the percolation phenomenon but a deeper analysis is

needed for the real application in the industrial operations.

In the first chapter, the influence of the segregation on the unit operiations in powder chemistry are shown.

In the second chapter, the mechanisms of segregation in the mixtures of granular materials and their reasons are explained.

In the third, the experimental procedures performed in the laboratory and the data analysis methods are carefully described.

And finally in the last chapter, the results of this work are shown; furthermore a new model which describes the percolation velocity behavior for the spherical particles is presented.

All the experiments of this work have been performed at the ATPLab (Advanced Particle Technology Laboratory) at Padova University.

Chapter 1

Importance of Segregation in Industrial Processes

1.1 Introduction

In process industry roughly 50% to 60% of the products are particulate (*R.N. Shreve and J.A Brink, Chemical Process Industries,1977*). The industries involved are several and very diversified: chemical pharmaceutical, food, minerals, fertilizers, plastics, energy production and many others.

Generally solids are more difficult to handle than fluids because their properties are complex. Indeed they can be characterized by properties of the single particles such as size, shape, density, surface area; and bulk properties which describe the behavior of a group of particles such as PSD (particle size distribution), bulk density, flowbility. Because of their peculiar behavior, unit operations which involve granular materials need to be studied carefully.

Granular materials tend to naturally segregate because of different mechanisms; one of these is called *Percolation*, it is a mechanism which permits to fine particles to move between a bed of coarser because of the voids they create in the bed.

There are several unit operations in the powder industries where percolation can cause segregation of the mixtures and this lack of homogeneity can be a problem when a certain quality degree in a product is desired:

1. *Mixing.* The goal of this process is to reach a certain homogeneity degree in agreement with the specification of the desired product. This unit operation is very difficult when granular materials are involved because they tend to segregate, so a lot of cares need to be taken, especially in the case of a balanced recipe or when a correct amount of an active pharmaceutical ingredient (API) is required. Indeed a too low amount of the active ingredient in a pharma can be ineffective, at the same time a too high amount can be toxic or lethal.

2. *Conveying*, which is the transportation of particles by fluids, liquids or gases. Different types of conveying are used in the industrial scale such as: hydraulic, pneumatic or mechanical. The particles are considered suspended in flow; but it is possible for them to slip in the fluid (if the fluid is faster than the solid particles) or to form two different regions: a diluite one, called also emulsion phase, which contains few particles above and a dense one of particles below. This heterogeneous flow depends on the particles and fluid properties and it is schematized in figure 1.1.

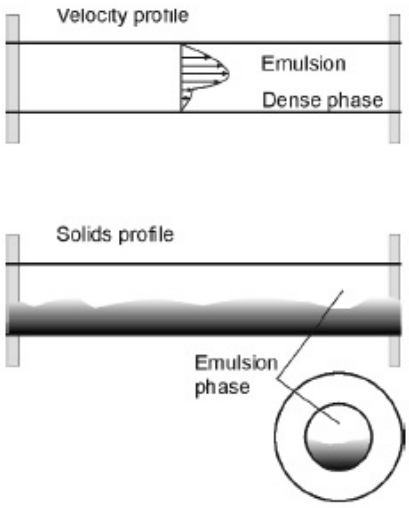

Figure 1.1: *Heterogeneous Flow in a Conveying Process and the respective velocity profiles of the Emulsion and Dense Phases.*

3. *Discharging* is a critic operation in silos where granular materials can be stored. A silo is made of a cylindrical or a rectangular upper part, which ends in a convergent part called hopper. The materials can flow in two regimes: mass flow and funnel flow. In the former, all the material is in flow, the velocity profile remains constant in the center, while close to the silo walls, it is characterized by the presence of velocity gradients and shear bands formations. In the latter, only the material which is on the discharge hole is able to flow and dead zones, where the material cannot flow, are created close to the silo walls; it is due to the slope of the hopper or the friction coefficient between the material and the walls. The material which occupied the dead zones can be discharged only when the silo is completly discharged.

   In a mass flow the fine particles can accumulate along the whole length

of the inclined walls, where the shear is higher and progressively exit from the hopper. During a funnel flow discharge, small particles can rapidly be accumulated in the hopper and remain there until the end of discharge: this can create a heterogeneous composition during the discharge time, where the coarse particles flow before the fines. In the following figure is shown the evolution of the segregation in two types of silos where the material flows in the two different regimes, obtained in a simulation. The scale of colors, from blue to red, indicates the increasing og the fines mass fraction.

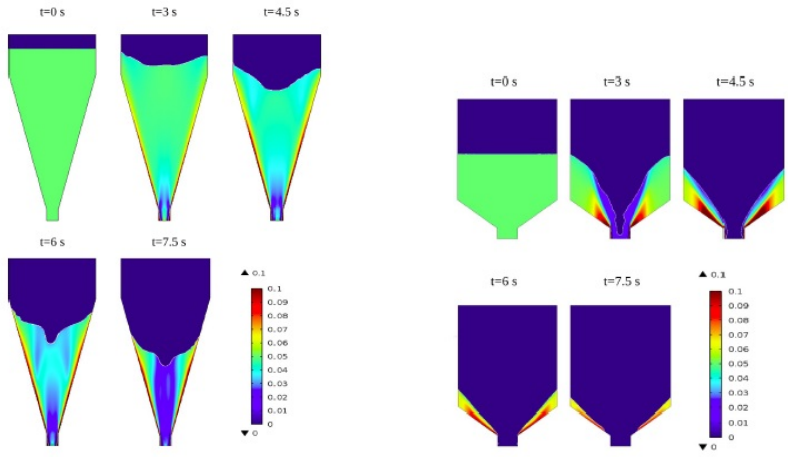

(a) *Mass Flow.* (b) *Funnel Flow.*

Figure 1.2: *Evolution of the Segregation in a Simulation of the Discharge of Silos in a Mass and Funnel Flows. (Bertuola et al., 2016)*

4. *Filling* occurs every time a vessel is charged with some granular material. Considering a system made of a binary mixture of coarse and fine particles where the free surface flows are dominant, the coarser particles are able to flow on the free surface while the fine particles are going to accumulate in the center of the vessel. Figure 1.3 shows a scheme of a bin filled with a mixture of two different sizes material.

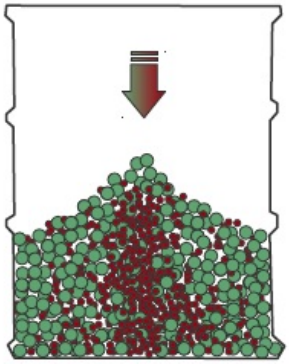

Figure 1.3: *Scheme of a bin filled with a binary mixture where materials differ from their size.*

Shinohara and co-workers (1979) studied this phenomenon: they concluded that the segregation process depends especially on the differing in size, shape and densities between particles; furthermore segregation was classified in three different stages:

- Penetration of smaller, more angular and denser particles through the voids of the framing particles.
- Sliding due to the entrainment between the upper flowing layer of the mixture and the lower stationary layer of the heap.
- Filling of the voids of the stationary layer with the separated particles.

All these operations are used daily in the industries. It is important to understand the causes and the behaviour of parameters which are crucial in segregation and percolation, to optimize the required quality of product. The segregation mechanism will be explained in detail in the next chapter.

1.2 Quality of a Mixture

The mixing granular materials are usually a critical operation in the processing industries but there are few studies about the equipment's performance and the effect of solid particle properties which are very different from the liquids. Mixing solid particles involves three different mechanisms:

1. Dispersion Mixing which is similar to the diffusion in fluids and where the motion of the particles depends on the random collisions between themself.

2. Convective Mixing that involves the movement of portion of matter.

3. Shear Mixing which is characteristic of powders.

We can distinguish between two classes of materials: cohesionless and cohesive materials. The materials of the first class are free-flowing and easy to handle, but problem during the mixing process could arise due to the differences in size, shape, density. Cohesive materials are characterized by the tendency to create agglomerates due to their physical and chemical properties.

The reason of the difference on the behavior of these two types of materials is due to the interparticle forces which act between particles such as: surface tension due to free interstitial liquid, electrical double layer,Van der Waals forces, strongly entangled particles, plastic deformation of particles caused by stress, which leads to local joining of particles.

If a mixture is composed by two types of particels in the same proportions, it is possible to distinguish different types of mixture (figure 1.4):

1. a *perfect mixture* where a sample of particles taken from any position in the mixture will contain the same proportions of each particle as the proportions present in the whole mixture.

2. a *random mixture* is a mixture in which the probability of finding a particle of any component is the same at all locations and equal to the proportion of that component in the mixture as a whole. It is the best quality mixture which can be achieved when there is not segregation.

3. a *segregating mixture* is the case where there is an higher probability to find one of the two component in one part of the mixture.

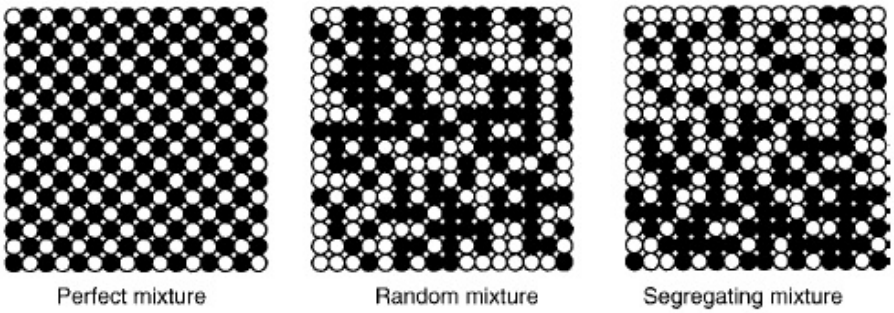

Figure 1.4: *Types of mixture.*

From a practical point of view a perfect mixture is never obtained. The aim of a good mixing process is to have a random mixture. The segregating

mixture is often obtained due to the difference in solid properties of particles such as shape, size and densities.

The true composition of a mixture, indicates as μ, is often not known; so it is necessary to find a mean composition $\hat{y}$, sampling the mixture.

$$\hat{y} = \frac{1}{N}\sum_{i=1}^{N} y_i \tag{1.1}$$

N is the number of sampling, and y_i is the composition of each sample evaluate from y_1 to y_N.

Because of their random behavior it is necessary to evaluate the second statistic moment: the variance. The true variance cannot be calculated exactly but it can be estimated using the correlations 1.2 or 1.3. It is used as a quantitative measures of the quality of a mixture.

$$S^2 = \frac{\sum_{i=1}^{N}(y_i - \mu)^2}{N} \tag{1.2}$$

$$S^2 = \frac{\sum_{i=1}^{N}(y_i - \hat{y})^2}{N-1} \tag{1.3}$$

The standard deviation is the root square of the variance.

For a two-component mixture the theoretical upper and lower limit can be defined. The completly segregated mixure variance, which defines the upper limit, is calculated as:

$$\sigma_0^2 = p(1-p) \tag{1.4}$$

where p and (1-p) are the propotions by number of the two components determinated from the sample. The lower limit can be obtaing using the equation 1.5 and represent a randomly mixed system.

$$\sigma_R^2 = \frac{p(1-p)}{n} \tag{1.5}$$

In the equation above n is the total number of particles in each sample. The figure **??** shows an example of how can change the variance s^2 in a mixture in the time. The variance is expressed in a logarithmic scale and it is possible to see that is included between the upper and the lower limits respectively σ_0^2 and σ_R^2.

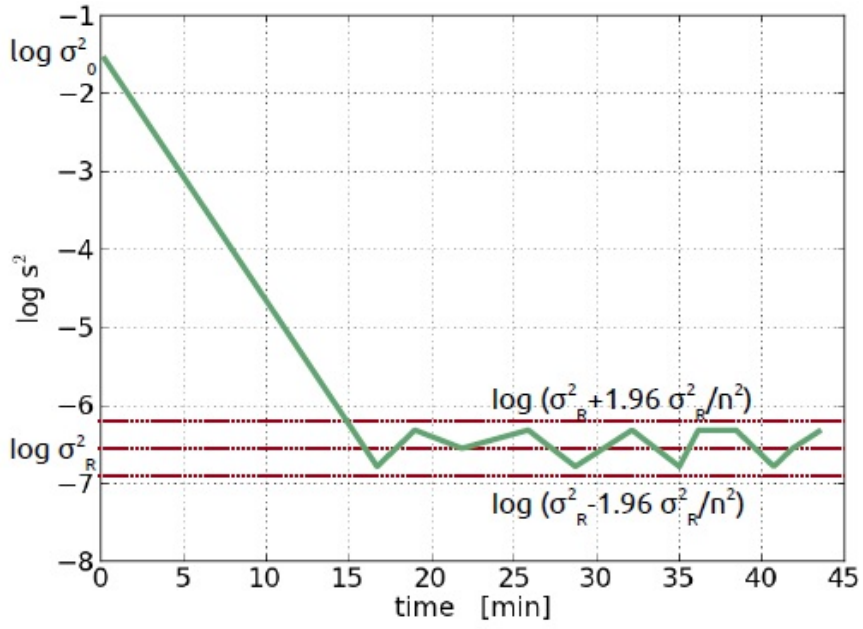

Figure 1.5: *Example of the evolution of the logarithm of the variance s in the time in a binary mixture* .

From the figure 1.5 it is possible to see that, after a certain time, the values of the variance are stable, but there is always a fluctuations due to the randomness of the mixture; they can be estimated using the correlation 1.6, which has a 95% confidence.

$$s' = \pm 1.96 \frac{s^2}{n^2} \tag{1.6}$$

Knowing the variances of completely segregated and random mixture, it is possible to define several different indices to evalute the mixture quality. The most used are the Lacey Mixing Index (LMI) or the Poole Mixing Index (PMI), which are respectively shown by the equations 1.7 and 1.8:

$$LMI = \frac{\sigma_0^2 - \sigma^2}{\sigma_0^2 - \sigma_R^2} \tag{1.7}$$

$$PMI = \frac{\sigma^2}{\sigma_R} \tag{1.8}$$

The LMI is the ratio between the achived mixing and possible mixing; when it is zero the materials are completly segregated, when its value is one, it means that the mixture is completly random. Practical values of the LCI are found to lie in the range between 0.75 and 1.

The Poole Mixing Index gives better discrimination for practical mixtures. It tends to the unity in the completely random mixtures. Many others Mixing Index exist in literature; so it is important to specify which index is used to assess the analysis (*Rhodes*, 1998).

1.3 State of Art

Particle percolation is a segregation mechanism which occurs when a small particle moves through the voids made by the larger bed particles, under the action of gravity and the shear. In figure 1.6 this mechanism is shown.

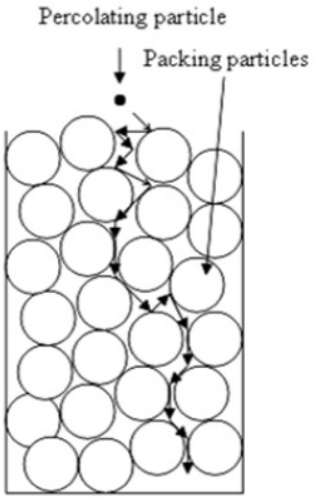

Figure 1.6: *Scheme of a Particle which percolate through a Packing Bed.*

Segregation mechanisms have been investigated using different methods, which can be divided in two main classes based on an experimental or a computational approach. Bridgwater and co-coworkers developed a Simple Shear Box which has been used to study the percolation speed of spherical glass particles; they demonstrate that the size ratio between particles is the most important quantity which affects percolation; in their studies a uniform, constant shear rate was assumed.

Puri, Duffy and co-workers (2010) have built a shear box, which is similar to the simple shear box used by Bridgwater, to study how the percolation velocity is correlated to the particle size ratio, strain rate and applied normal stress. They found that the percolation rate is influenced mainly by the difference in particle size, the normal stress does not have effect on the speed until is value is large enough to deform the bed particles. The strain rate is

also an important parameter especially when the size ratio between the fine and the coarse increases.

Another equipment developed for the percolation studies is the annular shear cell, which differently from the cells of Bridgwater and Puri, has the capability to produce a steady, uniform shear profile, without a transient phase. This cell has been used by Stephens and Bridgwater with tracer particles that were tracked by manually sampling material layer by layer in the cell.

From the computational point of view, three main approaches exist: Monte Carlo methods, Finite Element Method (FEM) and the Discrete Element Method (DEM).

Rosato *et al.* (1986) used a Monte Carlo algorithm to study the effect of the size ratio and the vibration amplitude in a segregation process.

Bridgwater, Savage and Lun (1989) developed one of the first theoretical continuum based percolation models.

Bridgwater and co-workers (1985) propose a model which was obtained by applying mass conservation of the particle species, incorporationg advective and diffusive fluxes, they have seen that comparing with the results obtained in the experiment using the annular shear cell the diffusive flux term is zero. The percolation velocity, used to calculate the advective flux, was an empirically derived function of the size ratio. Their model predictions compared well against experimental data, obtained using the simple shear cell, in the early time periods; for long time periods discrepancies occured, due to the semplification of their model.

Savage and Lun (1989) proposed a model to predict the segregation in a fully developed inclined chute flow. They assumed that the percolation was caused by: smaller particles falling through the random gaps between large particles and a size indipendent mechanism, which occurs for particles getting squeezed by neighboring particles out the giving layer.

FEM is based on the assumption that the granular materials can be described as a pseudo-fluid with a peculiar rheology. These models are used in the industrial scale, and require a low computing power.

Bertuola *et al.* (2016) presented a FEM model to predict the onset and evolution of segregation during the discharge of binary mixtures of granular materials. The model includes two different mechanisms: advection due to flow and segregation due to percolation; furthermore the effect of the particle size ratio and the initial fines concentrations are studied for different silo geometries, to investigate a funnel and a mass flow regimes, and compared with expermental data, finding a good agreement.

DEM simulations, differently from Finite Element Method, can study the particles motions singularly; the forces balance is applied to each particle of the examinated system. This algorithm is computationally more expensive but can provide detailed information about the micro-mechanics of the granular materials on the local scale. DEM are usually used when the number

of the particle is small, because of their high computationally costs. Khola and Wassgren (2016) used DEM simulation to develop correlations for the mean percolation velocity and the diffusion coefficient in a steady shear flow of a binary dispersed mixtures, using cohesionless, spherical particles. Fan and co-workers (2014) used DEM to provide a closure to their continuum model. They studied a geometry of a material flowing down a quasi two-dimensional heap, which is compared with their experiments. They back-fit to their segregation model's two dimensionless parameters to the DEM data for a range of conditions; so they could predict the experimental results.

The main methods used to study the segregation mechanisms, in the works which are listed, above will be described in detail in the following chapters.

Chapter 2

Mechanism of Segregation in a Solid Mixture

2.1 Introduction

Differently from fluids, granular materials are difficult to handle because of their characteristic shapes and sizes. In the previous chapter it has been shown how they are used daily in several operation and why it is important to know their peculiar behavior. Especially segregation, which is a phenomenon that characterizes all the granular material mixtures, can cause many troubles when a high degree of quality in the final product specification.

In the first part of this chapter the segregation mechanisms and their causes are explained. Then the attention will be focused on the percolation and the experimental and computational methods which have been used to study this phenomenon, which is the main topic of this thesis. Every methods has its own advantages and limits; so to analize in depth particle percolation, different techniques need to be used.

2.2 Segregation Mechanisms

The granular materials are characterized by the tendency to naturally separete during any industrial operation. This can cause problems if we want to guarantee a certain degree of homogenity in powder mixtures. The reasons of this phenomena are several but we can destinguish four main mechanisms which drive the segregation (identified by Williams,1990), which are schematized in figure 2.2.

1. Trajectory Segregation occurs when a small particle is projected horizontally with a certain velocity. It depends on the density of the particle and on the viscosity and density of the fluid. It is possible to define

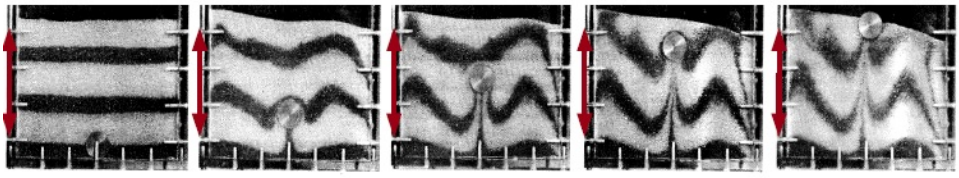

Figure 2.1: *Evolution of the motion of a disk of steel in a bed of glass particles due to vibration.*

a limiting distance x for the particle which can travel horizontally.

$$x = \frac{U \rho_p d_p^2}{18\mu} \tag{2.1}$$

where d_p and ρ_p are respectively the diameter and density of the particle, U is the velocity of the particle into the fluid, μ is the fluid viscosity and the constant 18 is due to the flux regime which is governed by the Stokes' law. This mechanism happens in pouring operation and in filling of containers where free surface flows are dominant. It occurs also in the end of a conveyor belt; indeed there is a method often used to divide the different types of plastics before the plastic recycle process which is based on this segregation mechanism.

2. Percolation of fine particles it is due to a rearrangement in the packing of the particles which can create gaps and permits to the particles above to fall and to some other particles to move upwords. It is striclty connected to the different size of the particles. This happens during the mixing processes or in charging and discharging storage hoppers.

3. Rise of coarse particles under vibration. If a mixture of particles of different size is exposed to vibration the larger particles move upwards. In the picture 2.1 is shown an experiment where a high size ball of steel is placed in the bottom of a box and covered by glass grains; they are put in order to form different colored layers so it is possible to see the evolution of the motion of the particles. When the box is shaked the steel ball rises to the surface. This phenomenon is called *Brazil-nut-effect* and has received many attention in the last years. The rise of the steel ball is due to the creation and filling of voids below it, due to the displacement of the small particles which compose the bed.

4. Elutriation segregation occurs when a powder containing an significant proportion of particles under 50 μm is charged into a hopper or a storage vessel and the air is displaced upwards. The upward flow of

the air may exceed the terminal freefall velocity of some of the finer particles, which are falling down; so they can then remain in suspension after the larger particles have settled on the surface of the storage vessel.

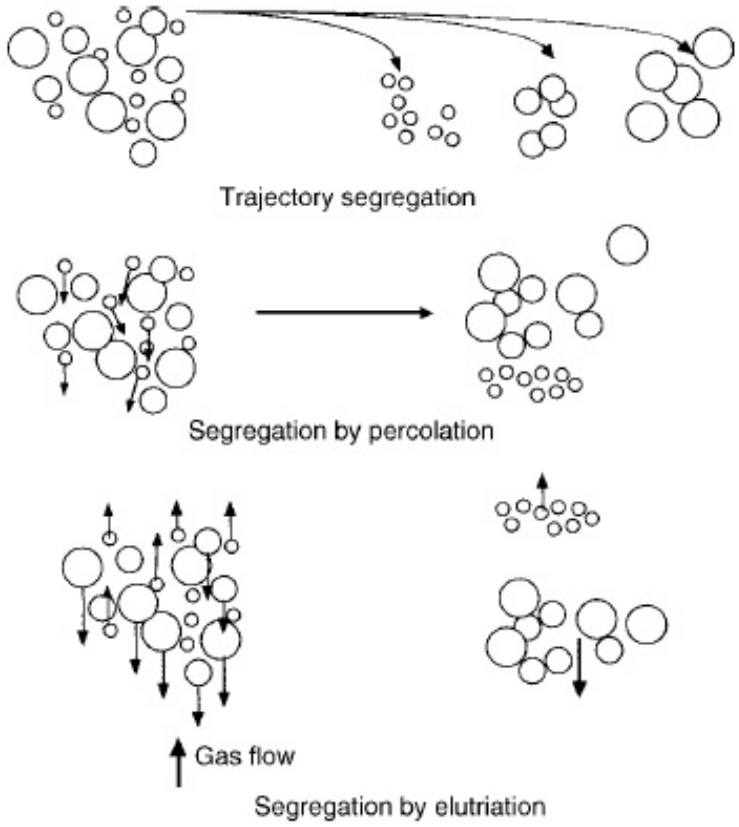

Figure 2.2: *Scheme of mechanisms of segregation in granular materials.*

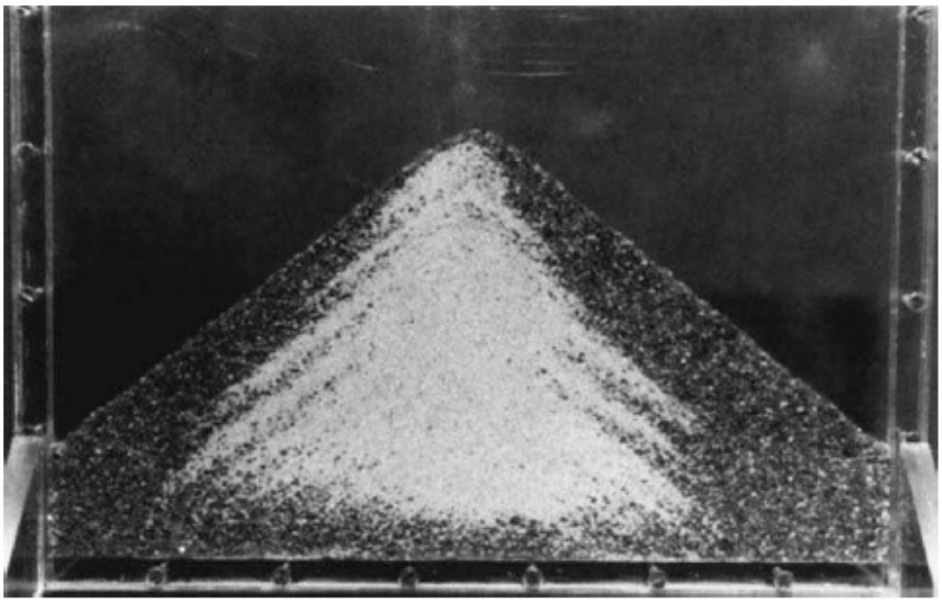

Figure 2.3: *Segregation pattern formed by pouring free-flowing mixture of two sizes of particles into a heap.*

2.3 Percolation

Percolation is a mechanism which permits to a fine particle to move between a bed of coarser because of the voids they create in the bed. Generally this is usually an unwanted phenomenon but it is present in a lot of unit operation such as: mixing, conveying, discharging, filling and storage compaction.

The fine particles need three main conditions to percolate:

1. the fines must be small enough to fit through the matrix which is formed by the void between the coarse particle.

2. Inter-particle motion or a strain must exist to allow the opportunities for fines to be exposed to multiple voids.

3. Fines need to be significantly free-flowing to pass through the pores.

Bridgwater (1985) and Khola (2016) defined two types of percolation: *Spontaneous Percolation* which may occur in absence of strain if there is a large size difference between particles, and *Shear-Iduced Percolation*. Khola, through a DEM analysis, has found a critical size ratio $d_p/d_b = 0.155$ in a

binary spherical mixture under which spontaneous percolation occurs and depends only on the action of gravity.

In figure 2.4 it is shown a sketch of fine spherical particles which percolate through a bed beacuse of the shear rate. The shear is perpendicular to the gravity; its directions are rapresented by the right and left arrows on the highlight picture.

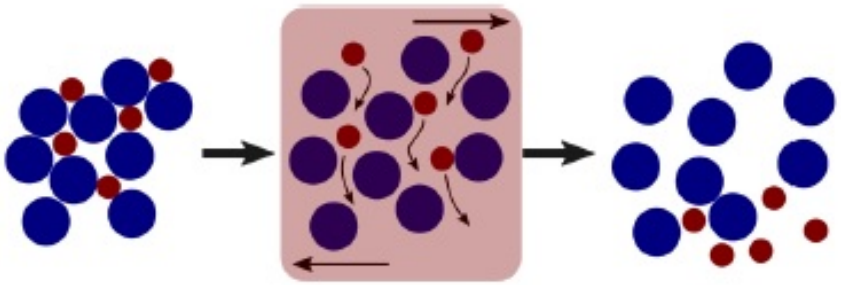

Figure 2.4: *Percolation of fine particles under shear condition.*

However the spontaneous percolation does not interest industrial application, and it is not usually investigated.

Bridgwater (1985) defined a dimensionless percolation velocity. It is function of many variables as it is shown in his equation 2.2, where the key physical quantities which can influence this phenomenon are shown.

$$\frac{u}{\omega d_b} = \frac{\hat{y}}{\gamma d_b} = f\left(\frac{d_p}{d_b}, \frac{\rho_p}{\rho_b}, R_p, R_b, \frac{\sigma}{E_b}, \frac{E_p}{E_b}, \frac{d_b \rho_b g}{E_b}, \frac{d_p \omega^2}{g}, \mu_b, \mu_p\right) \tag{2.2}$$

where u is the percolation velocity ω is the rate of strain, d_b is the bulk particle diameter, $\hat{y}$ is the mean distance percolated and γ is the shear strain. In the steady state the dimensionless percolation velocity is equal to the dimensionless displacement and it depends on a lot of variables which are listed and explained below:

1. $\frac{d_p}{d_b}$ is the ratio between the percolating particle and the bed particle diameters, is a measure of how the holes generated by the deformation of the bed are used by the fine particles.

2. $\frac{\rho_p}{\rho_b}$ is the ratio between the densities of the fine and the coarse particles.

3. R_p is the shape factor of the percolating material. It is important when there is a deviation from the spherical shape of the percolating material.

4. R_b is the shape factor of the bed material. It is important when there is a deviation from the spherical shape of the bed material.

5. $\frac{\sigma}{E_b}$ is the ratio of the normal stress to Young's modulus for the bulk material; it is a measure of the loss of free space,which can be used by the small particles to flow,it is due to the deformation of the bulk material due to the normal stress.

6. $\frac{E_p}{E_b}$ is the ratio of Young's moduli of percolation and bulk particles. This quantity is used to measure the loss of mobility of the percolating particle due to the deformation under stress.

7. $\frac{d_b \rho_b g}{E_b}$ where g is the gravity acceleration; it is used to measure the deformation of the bulk particle under its own weight.

8. $\frac{d_p \omega^2}{g}$ is the ratio between the time for a particle to fall through a gap and the lifetime of the gap under acceleration of gravity g.

9. μ_p is the dynamic coefficient of the percolating material; it is the measure of the frictional properties characteristic of the percolating material.

10. μ_b is the dynamic coefficient of the bulk material; it is the measure of the frictional properties characteristic of the bulk material.

2.4 Research Methods on Percolation

Percolation has been investigated in both computational and experimental methods, as it has been shown previously in the literature review. Because of the complexity and the randomness nature of this phenomeon almost all of the studies need to make several semplification. In this paragraph the most important methods used during the studies on segragation are explained in detail.

2.4.1 Computational Methods

Computational methods permit to simulate the behavior of many physical phenomena. Different methods have been used in the study of size segregation of granular materials. In this section the most important methods will be explained in detail, care will be paid on the models which have been used to describe percolation.

Montecarlo

Montecarlo methods are a class of computational alghoritms which rely on repeating random sampling to obtain numerical results. They are useful in many simulation systems with many degrees of freedom; they can be used for several applications such as: sensitivity analysis, in fluid dynamics for studying particular rarefied gas dynamics, in wind energy yield analysis and so on. Anyway the algorithm pattern followed is almost the same:

(a) The domain of interest is defined.

(b) An input of a random probabilty distribution is generated over the domain.

(c) A deterministic computation of the input is performed.

(d) The Results are aggregated.

This algorithm permits to reduce the computational costs during the analysis of a random phenomenon.

This method has been used to study size segregation and different granular dynamics by Rosato *et al.* (1979). However this method has some limitation: it does not have any physical time scale and the collision time is considered to be zero. It is difficult to relate the physical material properies to the granular dynamics, because the restitution coefficient has to be zero in order to minimize the potential energy during each particle movement. The Montecarlo technique has been reviewed to study the effect of the size ratio and the vibration amplitude in a segregation process. The system examinated is composed by a hard coarse disk which is sunk in a bed of small particles in 2-D. The configuration of the system of particles is denoted as:

$$r := (r_1, r_2, ..., r_n) \tag{2.3}$$

N is the number of particles; every particle has an energy $E_g(r)$ which is defined as the sum of the pair interaction terms equation 2.4 and the gravitational potential equation 2.5.

$$U(s) = \begin{cases} 0 & if s > d \\ \infty & if s < d \end{cases} \tag{2.4}$$

U is the pair of interaction which characterizes the disk: d is the disk diameter and s is the distance between theis centers. If the distance is

zero the repulsion force is infinite otherwise zero.

$$E_g(r) = \sum_{j=0}^{N} mgz_j \tag{2.5}$$

m is the mass of the disk and, g is the gravitational acceleration. To obtian the probability for a configuration r with energy $E(r)$ the Boltzmann distribution is used:

$$P[E(r)] = \frac{1}{Q} exp\left[\frac{-E(r)}{kT}\right] \tag{2.6}$$

Q is the partition function, k is the Boltzmann constant and T is the system temperature expressed in kelvin; furthemore the product kT is the measure of the kinetic energy of the system.

Particles move one at a time within a small neighborhood defined by a parameter $\delta > 0$. The disk position is denoted by the subscript j and his location is denoted by $r_j = (x_j, z_j)$, so its trial position is obtained by:

$$\begin{cases} x'_j = & x_j + \xi_x \delta \geq 0 \\ z'_j = & z_j + \xi_z \delta \leq 0 \end{cases} \tag{2.7}$$

where $\xi_x > -1$ and $\xi_z < 1$ are random numbers. In this way the trial configuration is generated. After that the energies are computed for the initial and the trial configuration. The new configuration is accepted unconditionally if the energy of the new state is decreased.

$$\Delta E := E(r') - E(r) < 0 \tag{2.8}$$

However, if ΔE is positive r' is accepted with probability:

$$P(\Delta E) = \frac{P[E(r')]}{P[E(r)]} = exp\left[\frac{-\Delta E}{kT}\right] \tag{2.9}$$

This value is compared with a random number ξ. If $\xi < P(\Delta E)$. the trial configuration becomes the new state otherwise it is rejected and the old configuration does not change. This procedure is carried out for all the N particles.

Finite Element Methods

Continuum models are often used in the industrial scale. They are computationally less expensive but also not very accurate, compared to discrete models; so usually they require many semplifications to describe the examinated phenomenon which do not reflect its real behavior. These methods consider the particles flow as a pseudo-fluid, and they are based on the solution of the conservation equation using CFD (Computational Fluid Dynamics) techniques. Because of this, systems which have a small number of particles cannot be modelled using this approach.

After the domain of study has been defined, it is divided in mesh so it is discretized and smaller control volumes are created. An example is shown in figure 2.5 where the boundary values of ϕ are the points A and B. The domain is divided in nodal points between A and B. The boundaries of control volumes are placed mid-way between the adjacent nodes; thus each node is surrounded by a control volume.

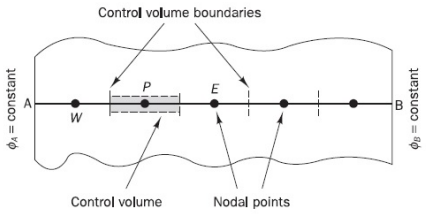

Figure 2.5: *Example of a control volume which is divided in mesh to be analyzed in 1-D* .

This operation is one of the most important because the meshes need to be set in a way to study as better as possible the examinated phenomenon. If the number of the mesh increases, the computational costs increases. This process can be done also in 2-D or 3-D; it depends on the phenomenon which needs to be studied (*H.K. Versteeg and W. Malalasekera, 2007*).

Then the mass conservation equation 2.16 is solved for every finite volume. It is discretized and it is found a solution for every mesh. In the case of granular materials the following equation is used to determine the volume fraction of the particles.

$$\frac{\partial C}{\partial t} + \nabla(Cv) = S \tag{2.10}$$

where C is the solid volume fraction, v is the solid bulk velocity and S is a source term that may be zero. The solid bulk velocity is an

important parameter which needs to be defined. For example, if v takes in account the gravitational force, the settling velocity will be:

$$v_{settling} = \frac{D^2 g(\rho_s - \rho_{air})}{18\mu_{air}} \tag{2.11}$$

where D is the particle diameter, g is the gravitational acceleration, ρ_s and ρ_{air} are respectively the densities of the particles and the air and μ_{air} is the air viscosity. Because it has been hypotized to study granular materials as a pseudo-fluid, the densities and the viscosities need to be defined in an other way; indeed the rheology of the granular material is very different compared to fluids.

Bertuola *et al.* (2016) studied *"Percolation in funnel and mass flow silos with an eulerian continuum approach"* where an Eulerian, continuum approach is used to describe a binary dispersed granular flow. The local mass fraction of the species in the mixture ω_i is calculated as:

$$\frac{\partial \omega_i}{\partial t} + \nabla(\omega_i v) = \nabla(J_{s,i}) \tag{2.12}$$

where $J_{s,i}$ is the segregation flux of the segregation velocity of the species i, the subscript i is 1 for the fine particles and 2 for the coarse particles. The segregation velocity of the species 1 has been assumed as:

$$v_1 = -K d_2 (1 - \omega_1)(\frac{d_1}{d_2} - 1)|\dot{\gamma}| \tag{2.13}$$

where K is a model parameter d_1 and d_2 are respectively the diameters of the fine and coarse particles, $\dot{\gamma}$ is the value of the shear rate and ω_1 is the fines concentration.

Discrete Element Methods

Discrete element methods (DEM) allow to simulate the real non continuum nature of the granular materials. They are very computationally expensive; since working with a huge number of particles can cause problems. In the DEM code, force balances are applied on the singular particles of the system; so it is possible to simulate the particles movement which is linked to the nature of the collisions. The total force

acting on each particles needs to be computated. The Newton's equation 2.14 of motion can be integrated numerically to find the velocity and the position of every particle at the current time.

$$m_i \frac{dv_i}{dt} = F_{total,i} \tag{2.14}$$

where m_i is the mass of the particle i , v_i is the velocity of the particle in the x, y, z coordinates, and $F_{total,i}$ are the total forces which act on the particles. They depend on the single phenomenon examinated. The second term of the equation 2.14 can be decomposed in:

$$F_{total,i} = F_{hydrodynamic,i} + F_{non-hydrodynamic,i} + \sum F_{contact,ij} \tag{2.15}$$

The hydrodynamic force takes in account the gravitational force and the drag and boyant forces applied by the fluid on the particle phase. The non-hydrodynamic force permits to consider the colloidal and capillary forces in the cohesive systems. The contact force is a term which needs to be evaluate. Generally the collisions involve two or more particles or one particle and the wall; they can be considered inelastic and can be estimated using the generalized spring-dashpot model:

$$F_{contact,ij} = F_{contact,n,ij} + F_{contact,t,ij} \tag{2.16}$$

where the two components are:

$$F_{contact,n,ij} = k_n \delta_{n,ij}^{\alpha} + C_n \dot{\delta_{n.ij}} \tag{2.17}$$

$$F_{contact,t,ij} = k_t \delta_{t,ij}^{\beta} + C_t \dot{\delta_{t.ij}} \tag{2.18}$$

The first and the second terms of the equations 2.17 and 2.18 represent respectively the repulsion and the dissipation forces, $\delta_{n,ij}$ and $\delta_{t,ij}$ are the normal and the tangential components of a small overlap between the contacting particles i and j, k_n and k_t are the stifness coefficients, while C_n and C_t are the damping coefficients and α and β the parameters.

The figure 2.6 represents the simulation of a Simple Shear Cell, it uses an open-source DEM software called LIGGGHTS (stands for LAMMPS improved for general granular and granular heat transfer; where LAMMPS is a classical molecular dynamics simulator) by Khola and his coworkers (2016); which is coded in a python language. The cell has a fixed lenght in the x direction and a fixed width in the y direction.

Parameter	Value
Coarse Particles Elastic Modulus E_c	5 MPa
Coarse Particles Poisson's ratio ν_c	0.3
Fine Particles Elastic Modulus E_c	5 MPa
Fine Particles Poisson's ratio ν_f	0.3
Coarse-Coarse Coefficient of restition ϵ_{cc}	0.2
Fine-Fine Coefficient of restition ϵ_{ff}	0.2
Fine-Coarse Coefficient of restition ϵ_{fc}	0.2
Coarse-Coarse sliding friction coefficient μ_{cc}	0.4
Fine-Fine sliding friction coefficient μ_{ff}	0.4
Fine-Coarse sliding friction coefficient μ_{fc}	0.4

Table 2.1: Summary of the values of the parameters used during the DEM Simulation of Khola and co-workers (2016) to charaterize the particles of the system.

The upper and the lower wall boundaries consist in glued spheres of diameter d_c arranged in a square lattice without overlap, they are colored in red in the figure, they behave as a sieve and allow to the fine particles to pass through but not to the coarse. Periodic boundaries conditions in the x and y directions are fixed. The height of the bed can vary, adding a normal stress σ which acts on the top of the bed. The height of the cell in its initial position is set to 8 d_c but it varies depending on the shear rate. The upper and the lower layers are moved in the opposite direction in order to generate a velocity gradient ω within the bulk particles.

The fine particles are set as a single row of boundary spheres spaced of 4 d_c in the x direction and 1 d_c in the y direction in order to produce a linear velocity profile in the bulk.

The materials properties: elastic moduli, Poisson's ratios, coefficients of restitution, and sliding friction coefficients are summarized in the table and are held constant during the simulation.

During the simulation cohesive and fluid forces are excluded. The gravity acts in the negative z directoin, only on the fine particles.

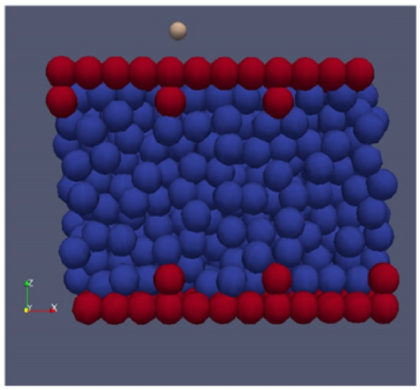

Figure 2.6: *Image of a Shear Cell simulation using a DEM code called LIGGGTHS .*

2.4.2 Experimental Methods

Percolation has been investigated experimentally using different equipments. This type of analysis has many technical problems, it is very difficult to create an equipment which can generate a controlled percolation to permit a quantitative analysis. In this section three different shear cells will be described to see their principles of functions, their advantages and dis-advanteges which were used in the design of the simple shear cell accounted for in the APTLab during the experiments.

Simple Shear Apparatus

The first simple shear cell has been built by Bridgwater (1985) to study qualitatively and quantitatively the percolation; after many renovation, the final box called Mark IIA, shown in the figure 2.7 has been made. It is a box which can turn its cross section from a rectangle to a parallelogram. Two side walls are fixed to a Perspex cell; they are hinged at the bottom and connected together at the top, using two bars. The walls motion is controlled using a gear; so they can move and are capable to produce large strain. The lid is free to float on the top of the bulk material. The dimensions of the box are 354 mm in the direction of the motion by 355mm wide by 269 mm heigth, when the hinged walls are vertical (maximum bed height). The base plate of the box, consists of 33.1 mm diameter hemispheres cemented to a metal tray. Holes are drilled between the hemispheres, in a way to create a sieve where the fine particles are allowed to pass through. The box contains a bed of coarse particles. The percolation particle enters the bed through a tube which is inserted in the lid with a trap door and

the timer is started. Under the cell lay a metal plate to which a microphone is connected. When the particle hits the tray, a pulse stops the timer and the elapsed time is recorded. Phenolic resin spheres, 38.1 mm in diameter, are drilled and fixed on the rods. The arrangement of the spheres is chosen to allow particle up to 15 mm in diameter to fall spontaneoulsy. Gear wheels are located on the ends of the rods and as the base moves the gear runs along the fixed rack. The microphone is connected to a signal-conditioning unit so that, when a particle falls from the cell into the bottom tray, the elapsed time and channel is recorded.

A disadvantage of this device is that is not possible to produce a steady uniform shear, but because of the construction characteristic, a transient regime exists necessarily.

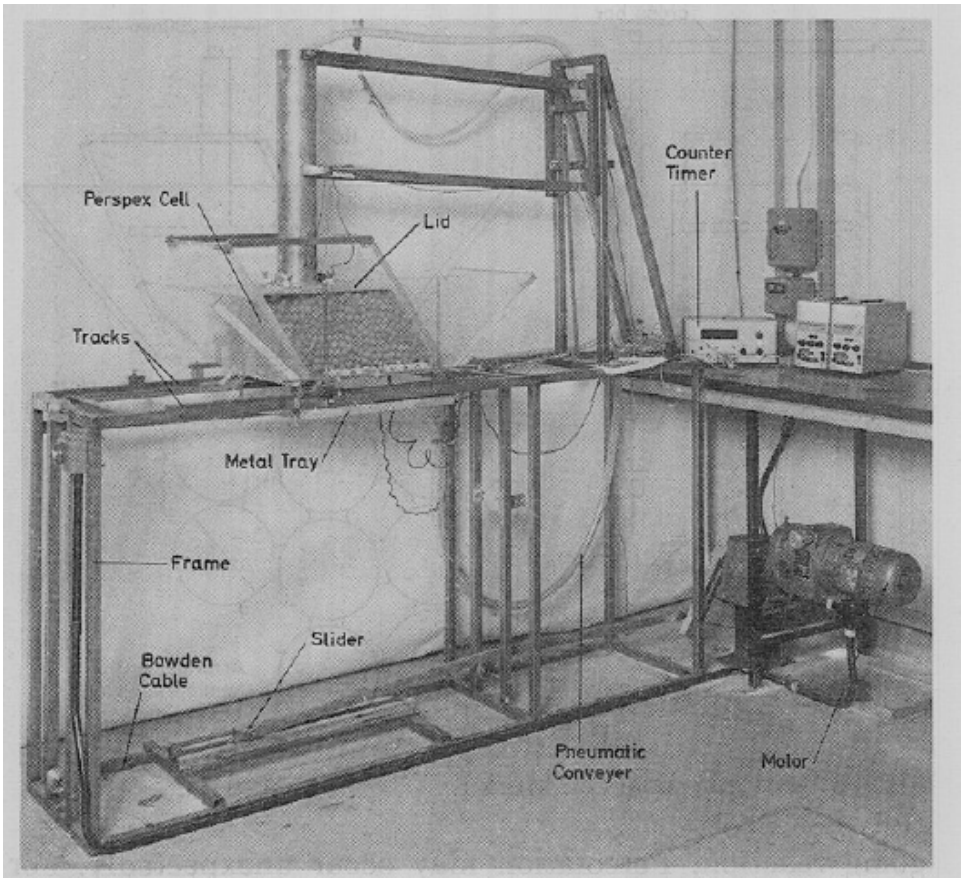

Figure 2.7: *Experimental Simple Shear Apparatus Mark IIA built by Bridgwater and his Co-workers.*

Puri and his co-workers (2014) built a simple shear cell, which is similar to the Bridgwater box, called PSSC II (*Primary Simple Shear Cell*). Their equipment is shown in figure 2.8. It consists of five main parts: shear box, sieving system, measurement system, drive system and main frame.

The shear box provides shear motion in a way to simulate the percolation. The sieving system is placed at the bottom of the shear cell and has the function to separate the fine percolating particles, which are accumulated at the lower part of the mixture. The drive system provides enough power to impose the strain that the test material, which is loaded in the cell, requires. The measurement system is able to measure percolated fines and distributions of fines. Finally the frame is used as a stable support to the other systems and guarantee enough space for the operation.

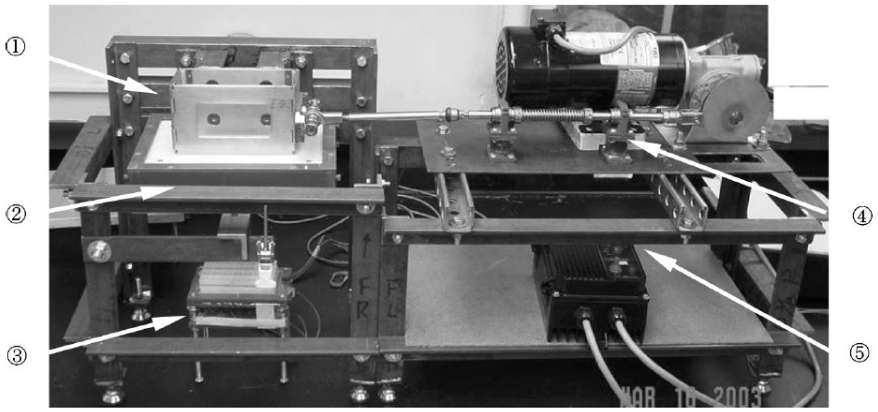

Figure 2.8: *Fabricated and assembled PSSC.II; 1, Shear Box; 2, Seiving System; 3,Measurement system; 4, Drive System; 5, Main Frame.*

The shear box has a rectangular shape and its dimensions are 150 mm in length, 63 mm in width and 100 mm in height. Differently from the Bridgwater cell, the PSSC II can provide the shear motion in the x directon. Indeed three principale motion directions along the x, y ,z axis can be chosen; as it is shown in figure 2.9. When the shear motion occurs along the y-axis, clearly the bed particles close to the bottom of the shear box receive zero energy from the moving side walls. A horizontal zero energy zone which is perpendicular to the gravity (along the z axis), can also affect the experiments of percolation. Because of the existence of these dead zones, the best choice is to create the shear motion along the x-axis (figure 2.9(c)). From the geometrical point of

view, the volume of the shear box decreases when the box is sheared.

The measurement system consist of four load cells, configurated along a row where a square platform is attached to each load cell. This is capable to collect fine particles within an area of 169 mm^2, which is the 3,4% of the total screen slot area. So the segregated mass of fines that each load cell measures can be considered approximately as point measurement.

The fine particles are fed on the top of the particle bed contained in the cell, with an opening size 3.9 mm. It is placed at the interection of the two diagonals of the rectangular shear box.

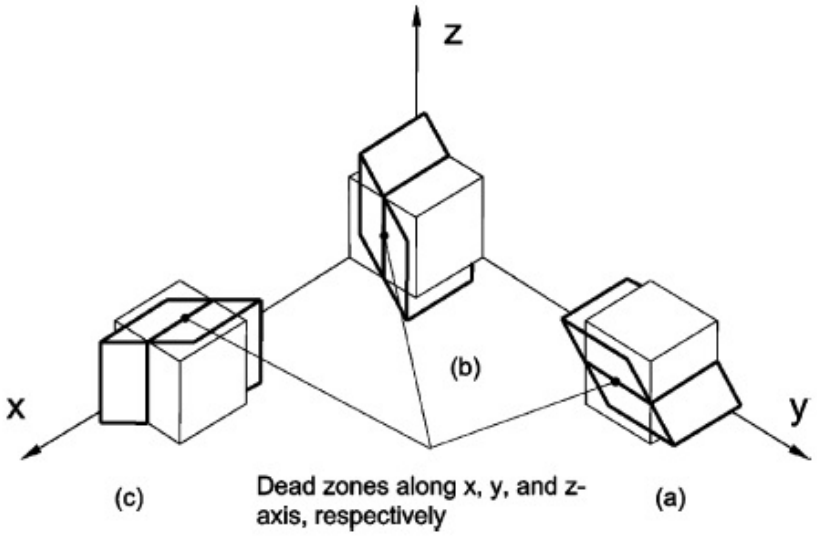

Figure 2.9: *PSSC II possible shear motion selection based on the different position of the dead zones: (a) along y-axis, (b) along z-axis, (c) along x-axis.*

Annular Shear Cells

The annular shear cells have the advantage of being able to produce steady, uniform shear profiles without the transients and un-limited strain. The first apparatus has been built by Stephans and Bridgewater. A simple scheme is shown in figure 2.10 (a). This cell can confine the particles between a top plate which is free to move vertically and a rotating bottom plate. The radius of the inner wall of the cell is 25.5 cm and the width of the particle-filled channel is 3.8 cm. The top and the bottom plates are lined with rubber to increase their friction coefficient, while the sidewalls are bare with alluminium. The bottom

plate can rotate to a frequency of 49 mHz creating a shear band which extends a few particle diameters into the cell. The pressure of the cell is adjusted using two techniques: weighing the top plate to increase the normal stress or partially suspending the top plate in a way to reduce the pressure on the granular material.

In the pictures from 2.10 (b) to 2.10 (d) the evolution of an experiment is shown: at the beginning, two layers of particles are charged. The small particles are placed on the upper part of the annular cell and the coarse close to the bottom. During this experiments, glass spheres with identical densities are used. When the shear strain begins, the small particles fall down through the large particles. At the end of the test, all the large particles have reached the top of the cell and form a re-segregating mixture where the layers are placed in the opposite way respect their initial position.

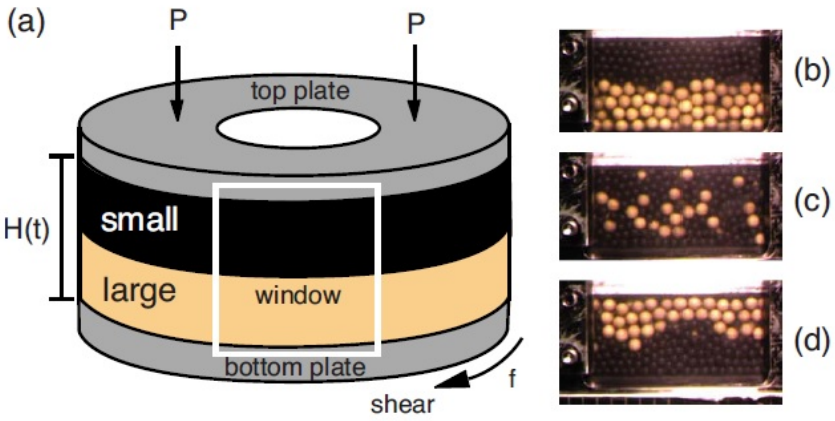

Figure 2.10: *(a) Scheme of the Annular Shear Cell in its initial configurations of particles. (b) Initial configuration. (c) Mixed state. (d) Final Re-segregated state.*

Chapter 3

Experimental Procedure and Data Analysis

3.1 Introduction

This chapter is divided in two sections: in the first section the experimental procedure performed in the laboratory is explained and all the equipments which are used during the tests are carefully descibed. In the second section the data analysis procedure used to calculate the percolation velocity and the diffusion coefficent are explained. All the calculations are made using Matlab codes.

3.2 Simple Shear Box Construction and Improvement

To quantitatively study the percolation, an equipment called simple shear box has been built. This shear apparatus is similar to the the simple shear box used by Bridgewater (1985) during his experiments.

The simple shear box is an equipment which contains a test materials and is able to switch from a cube to a parallelogram; in this way it is possible to strain the particles which are inside it. In figure 3.1 a schematic picture of the box is shown, drawn with AutoCAD.

During the experiments three main constrains, defined by Bridgwater (1985), must be respected to permit a fine particle to move through a bed of coarser ones:

1. the fines must be small enough to fit through the matrix which is formed by the voids between the coarse particle.

2. Inter-particle motion or a strain must exists to allow the opportunities for fines to be exposed to multiple voids.

3. Fines need to be sufficiently free-flowing to pass through the voids.

In the picture3.1, it is possible to see the two main parts of the cell: the red walls form the "body" and are fixed, the blue lateral walls are hinged to the body of the box and are able to rotate from a vertical position of 90° until they reach the desired angle of 45°. The lateral walls are connected together so they must move together. The axes of the system are set as z the height, y the width and x the lenght of the shear box, they are shown in the figure 3.1. The test material is charged in the shear box and subjected to the shear stress, generated by the wall motion. The bed particles are forced to move in the x direction. The principle of operations of the simple shear box is shown in the figure 3.2.

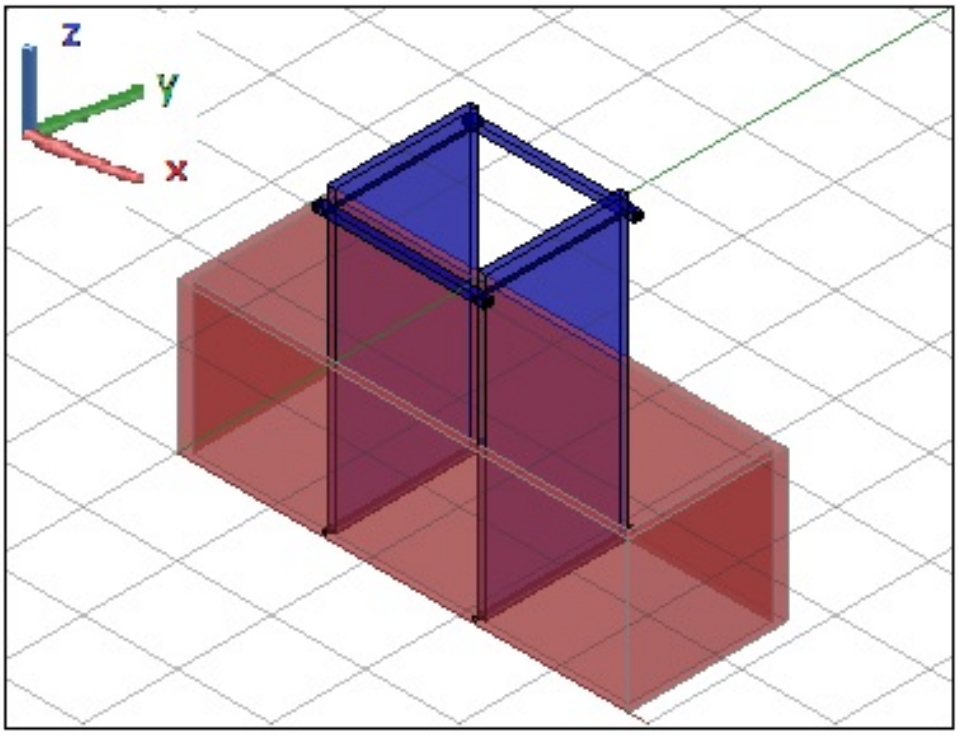

Figure 3.1: *3D Shear box picture, drawn with AutoCAD.*

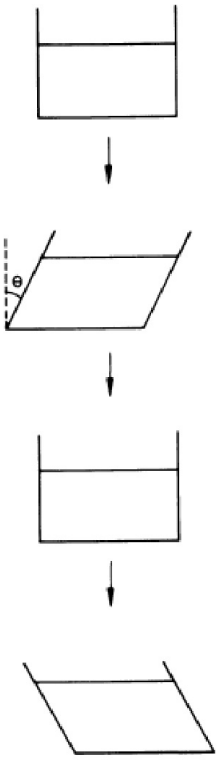

Figure 3.2: *Principle of operation of the Simple Shear Cell: the walls of the box are able to move until they reach a certain angle θ.*

The box is made of wood and there is a transparent bottom made of plexiglass which allows to see the small particles after they are percolated through all the bed of coarser ones. The dimensions of the simple shear box when the mobile walls are in vertical position are 10x10x10 cm.

To see better the small particles when they arrive to the bottom of the box, they have been colored with different colors so it is possible to see clearly the contrast between the bed particles and the percolated one.

After preliminar tests, it was possible to see that, because of the construction of the box, the lateral walls were not able to move all the bed in the same way. In particular the layers close to the bottom of the cell could not move at all, so it was necessary to raise the bed of 8 mm from the bottom; that was possible adding a plexiglass plate inside the box. It was transparent so it is anyway possible to see particles when they cross all the bed. Furthemore using friable material, the internal walls of the apparatus were covered with a metal sheet, otherwise some particle of the test material could break up and get stuck in the opening between the fixed and the mobile walls, causing a malfunction of the box. Indeed they can interlock in

Material	Shape	Size [cm]
Polyethylene	Spherical	0.6
Glass	Spherical	0.5
MCC grains	Irregular	0.45
MCC grains	Irregular	0.38

Table 3.1: *Beds used during the tests.*

the free space between the mobile and the fixed walls.

It has been observed that during the experiments, an undesired recirculation of the particles affects the surface of the bed; to avoid this phenomenon, which could affect and un-validate the results, a lid has been built; it is made of plexiglass and has two baffles which can penetrate on the particle bed limiting the re-circulation of the particles that compose the upper part of the bed.

3.3 Experimental Procedure

The experimental tests have been performed using two different methods. Indeed during the experiments an undesired mixing effect on the upper part of the simple shear apparatus significantly affected the measurements. In order to avoid this effect the measurement method needed to be changed.

3.3.1 Method 1

The experiments were performed using different test materials: glass and plastic spherical particles and irregular granulated particles made of flour and MCC (Microcrystalline Cellulose), which were made using a High Shear Granulator.

The tests have been performed changing the velocity of the walls motion and the diameter ratio of the particles. Four different frequencies have been chosen respectively 0.25, 0.5, 0.75, 1 Hz in a way to generate four different shear respectively 0.66, 1.35, 2.02, 2.70 s^{-1}.

Different size ratios are obtained keeping the size diameter of the bed particles constant and varying the size of the fine particles. It was seen that the bed particles size were relevant in the percolation speed measurement; so the percolation velocity can be compared only if the bed particles size is the same. The beds used during the test are summarized in the table 3.1.

Here the steps of the procedure used to perform all the tests are reported:

1. Measure the weight of the particles which make up the bed using a balance.

2. When a mixture of spherical particles is used a low quantity of smaller sphere is added; they are placed at the bottom of the box; they have different size but they are still big enough to guarantee to small particles to percolate. In this way all the upper layers will have a displacement and it is possible to create a "lack" of the ideality of the system.

3. Charge the shear box: the last layer is placed on the bottom and then it is covered with all the other spheres which form many layers on it.

4. Measure the height of the bed using a yardstick: it has been set to 7.4 cm.

5. Place the fine particles in their initial position on the top of the shear box. During one test, four particles which have different colors are placed to the same distance from the mobile walls.

6. Take a picture of the initial positon of the particles.

7. Add a cover.

8. Start to move the walls of the box and measure the percolation time with a cronometer. The frequency of the motion of the walls is kept constant in each experiment. When the test begins motion walls position of the simple shear apparatus must be vertical.

9. When all the particles are percolated, take a picture of the bottom of the shear box.

10. Discharge all the particles from the cell.

11. In the end the particles which are used during the test are sieved to separate the small particles from the coarser ones.

3.3.2 Method 2

Because of the simple shear apparatus construction characteristics the upper part of the cell where the test material is charged is affected by an undesired mixing effect; which compromizes the measurement during the tests. A lid made of plexiglass has been added to reduce this effect but still there were issues during the measurement; so it has been decided to keep constant the height of the bed and reduce the height of the percolationg particles initial position. In this way the recirculation of the particles on the surface of the bed does not affect the measurement. The steps of this new methods are now reported:

1. Measure the total weight of the particles which make up the bed using a balance.

2. The bed is charged in the simple shear apparatus up to a height of 4 cm. The height is measured using a yardstick.
3. Take a picture of the initial positon of the particles.
4. Place the fine particles in their initial position on the top of the shear box. During one test, four particles which have different colors are placed to the same distance from the mobile walls.
5. Cover them with the rest of the bed particles up to a height of 7.4 cm.
6. Add the lid to close the simple shear box.
7. Start to move the walls of the box and measure the percolation time with a cronometer. The frequency of the motion of the walls is kept constant in each experiment. When the test begins motion walls position of the simple shear apparatus must be vertical.
8. When all the particles are percolated, take a picture of the bottom of the shear box to see their final position.
9. Discharge all the particles from the cell.
10. Separate the particles used during the test using a sieve.

To verify that the fine particles do not start to fall between the bed voids during the charge of the second part of the bed in the box, a quasi-2D static cell has been used. It is composed by a 2 glass walls so that it is possible to see the particles position. It has been filled with the bed particles for half of its height; then the fine particles are placed close to the glass wall and their position has been marked. The rest part of the bed is charged in the cell. Finally the position of the fine particles has been checked to ensure that they could not percolate through any bed particle layers; it was seen that fine particles does not percolate during the second charging phase.

3.4 MCC Particles Production

The particles with irregular shape were made in the laboratory using a granulation process and then sieved.

3.4.1 Granulation

The Granulation is a process where the primary particles are stuck together so it is possible to build particles with a higher dimensions.This technique is used in the several industries such as food and pharmaceutical to improve the physical and chemical properties of particles.

To produce the new particles the following procedure was used (see figure 3.3) and it consists in three main phases:

1. Wetting: the powders are charged in the granulator and are mixed adding the binder which permits to form interparticles bonds.
2. Granulation: adding a binder and increasing the mixing velocity of the impeller, a homogenous mixture of grain is obtained.
3. Drying: the liquid is separeted by evaporation so the particles which have been generated becomes stable.

Figure 3.3: *Granulation Procedure.*

The tested granular material has been obtained in the laboratory, using the following procedure:

1. A flour and Microcrystalline Cellulose mixture is loaded in the granulator in the same proportion for a total amount of 300 g.
2. A dry premixture is performed at low speed of the impeller (300 rpm) for 3 minutes.
3. Water is added using a peristaltic pump. It is addes in the same amount of the powders (300g).
4. The impeller speed is raised up to 1200 rpm and this velocity is kept constant for approximately 4 minutes.
5. The product is discharged and dried in the oven at 60°C for two hours.

Size [mm]	Weight [g]	Δd_i	w_i	w_i/d_i	F_i
<1.4	28.14	1.4	0.015	0.01	0.015
2.0-1.4	167.5	0.6	0.09	0.15	0.105
2.8-2.0	260.48	0.8	0.140	0.175	0.246
3.3-2.8	256.77	0.5	0.0138	0.277	0.384
4.0-3.3	397.46	0.7	0.214	0.306	0.600
5.0-4.0	461.7	1	0.015	0.249	0.848
>5	247.83		0.133		0.990

Table 3.2: *Sieving Results.*

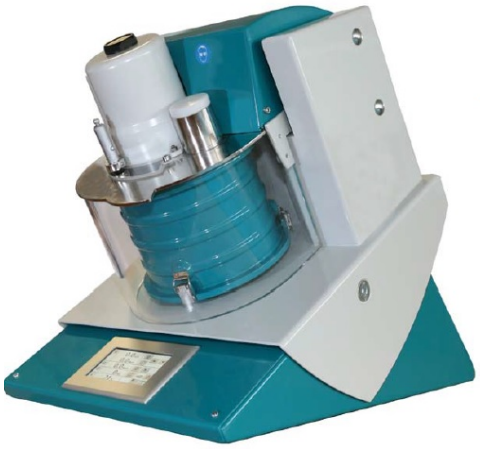

Figure 3.4: *High Shear Mixer Eirich EL1 used in the laboratory during the Microcelluse particle production.*

3.4.2 Sieving

The granulated particles are then separated using different mesh size sieve. Six different square mesh size sieve have been used to separate higher size particles from fines. The material is placed on the top mesh of the device, which is shown in the figure 3.5 and a certain vibration amplitude is applied for few minutes; so the fine particle are able to pass through the sieve holes while the coarser cannot and the particles are separated for their characteristic size.

In the end of the operation, the quantity of material contained in each sieve is weighed; in this way it is possible to obtain a Particle Size Distribution (PSD). In the table 3.2 the results of the sieving operation have been reported.

In the table Δd_i is the characteristic sieve size measured in mm, w_i is the material weight fraction, w_i/d_i is the normalized material weight fraction

and F_i is the cumulative weight fraction.

Figure 3.5: *Sieving used in the laboratory.*

The final differential and cumulative particle size distributions of the granulated material are reported in the figure 3.6. During the tests two different beds made of MCC grains were used, their mean sieve diameter size were respectively 0.38 cm and 0.45 cm; furthermore smaller particles were chosen in order to have different ratio diameters.

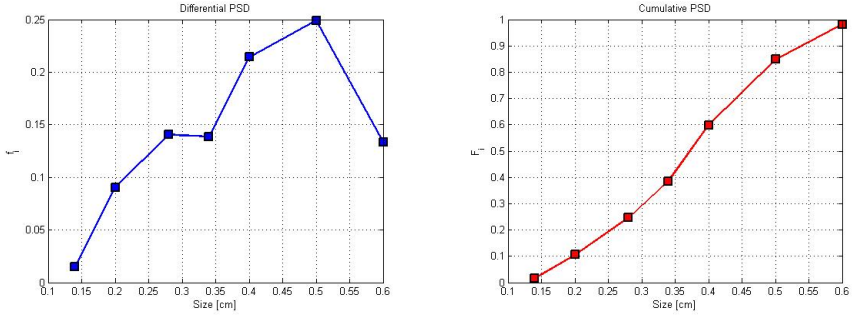

(a) *Differential Particle Size Distribution.* (b) *Cumulative Particle Size Distribution.*

Figure 3.6: *PSDs of the granulated particles.*

3.5 Materials Characterization

In this section it is explained how the properties of granular materials were measured; furthermore the results of the measurement of the true density, bulk density, shape and internal friction coefficient are presented.

3.5.1 True Density

The true density of a granular material is the density of a powder, where the volume is measured not taking to account the open and the close pores. It is not very easy to measure the mass and the volume of a single particle. The pycnometer is an equipment used to measure the true density.

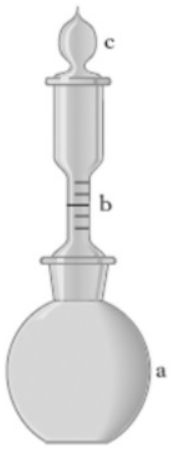

Figure 3.7: *Pycnometer.*

In the the figure 3.7it is possible to see the device divided in its main parts: (a) a glass bin, (b) a capillary pipe where a mark is drawn, (c) a cap.

The procedure, which is schematized in the figure 3.8, consists in the measurement of four different weights. It was done using an electronic scale.

1. At first the weight P1 is measured to set the tare.
2. In a second moment the measure of P2 is taken, which is the weight of the sample of the analyzed material.
3. Then a liquid is added, which has a known density, and P3 is measured ; the pyncometer has to be filled with the liquid until the reference point.
4. Finally It is taken the weight of the liquid which occupied all the reference volume, P4. It is important that all the air bubble in the system flows out, to obtain a good measurement.

	Polyethylene	Glass	Grains
solid	15.72	28.91	4.59
solid+liquid	110.15	123.4	52.83
liquid	105.93	105.93	51.39
mass	611.4	1085.1	443.1
volume	748.8	707.2	756.0
ρ_{true}	1362.9	2519.5	1340.6

Table 3.3: *True Density Results.*

After these mass measurements are taken, it is possible to determine the solid, reference liquid and mixture masses as:

$$m_{solid} = P_2 - P_1 \tag{3.1}$$

$$m_{liquid} = P_4 - P_1 \tag{3.2}$$

$$m_{tot} = P_3 - P_1 \tag{3.3}$$

Finally the true density can be obtained, using the reference liquid density ρ_{liquid} in its standard conditions.

$$\rho_{true} = \rho_{liquid} \frac{m_{liquid} m_{solid}}{m_{liquid} + m_{solid} - m_{tot}} \tag{3.4}$$

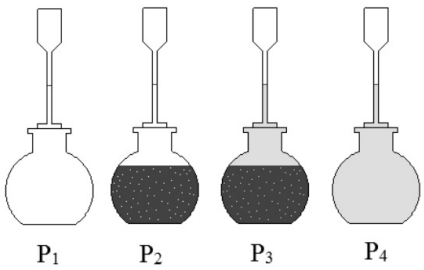

Figure 3.8: *Schematic Procedure of Pycnometer Uses* .

To measure the glass and polyethilene density, water has been used as a reference liquid; while to measure the true density of the MCC grains, silicon oil, which is an apolar liquid, has been used, because of their solubility in water. The results are shown in the table 3.3, where the mass values are expressed in kg and the volume in m^3.

3.5.2 Bulk Density and Bed Porosity

The bulk density ρ_{bulk} is a property of a powder in bulk. It is not an intrinsec property of the material and it is defined as the mass of many particles of the powders and the total volume they occupy. The volume includes the particle volume considering their pores and the inter-particle void volume.

The bulk density has been measured directly in the shear box, where a certain quantity of a test material is weighed and charged in the cell. The lengths of the cell walls in the x and y axis are known, so the surface of the bed has been measured using a yardstick. Because the height of the bed is not flat several measurements have been made and an average value is taken to calculate the total volume that the test material occupied.

Finally the bed porosity ϵ has been obtained as:

$$\epsilon = 1 - \frac{\rho_{true}}{\rho_{bulk}} \tag{3.5}$$

The results are shown in table 3.4, the values of the densities are expressed in kg/m^3.

	Polyethylene	Glass	Grains
ρ_{true}	1362.9	2519.5	1340.6
ρ_{bulk}	816.5	1534.4	586.2
ϵ	0.40	0.39	0.56

Table 3.4: *Bed Porosity Results.*

3.5.3 Coefficient of Static Friction

The coefficient of static frictions of the grains has been measured using the static response angle, while for the glass and plastic spheres literature values have been chosen.

The static response angle α is defined as the angle between the free surface of a powder heap and an horizontal plane. It is shown in figure 3.10. The angle depends on the nature of the surface of the material flows. This angle is used to measure the flowbility of granular materials. For free-flowing materials it is equal to the arctangent of the coefficient of static friction μ_s *(Neddermann, 1995).*

$$\mu_s \approx tan\alpha \tag{3.6}$$

Figure 3.9: *Static response angle definition.*

The equipment used to measure the static response angle is shown in the following figure. The material flows through a hopper placed at a certain height until the heap is formed. In the horizontal plane is placed a paper sheet with concentrical circles drawn on it. The center of the circles corresponds to the hopper hole. The pile diameters of the materials are measured and the mean value is taken. The static response angle is calculated as:

$$\alpha = tan^{-1}\frac{2h}{D-d} \tag{3.7}$$

where h is the height from the horizontal plane to the hopper outlet, d is the hopper die diameter and D is the mean diameter of the heap base.

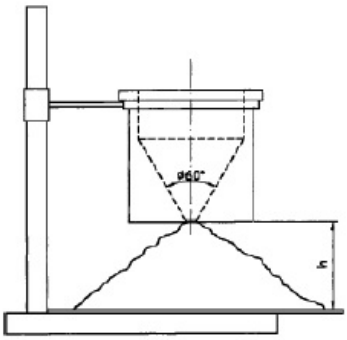

Figure 3.10: *Equipment used to measure the static response angle.*

The results of this analysis are summarized in the the table 3.5

3.5.4 Shape Analysis

The characteristic shape of the granulated particles have been measured using image analysis. Eighty particles have been scanned, their characteristic size properties have been calculated using a software called Image Tools. Before performing the image analysis the software needs to be calibrated

Material	Diameter Size [cm]	Response Angle α	Coefficient of Static Friction μ_s
Polyethylene	0.6	23.4	0.43
Glass	0.5	23.4	0.43
MCC grains	0.45	27.97	0.53
MCC grains	0.38	32.55	0.64

Table 3.5: *Coefficient of static friction of the bed materials used during the tests.*

using a graph paper. In figure 3.11 a scan of the MCC granulated particles is shown.

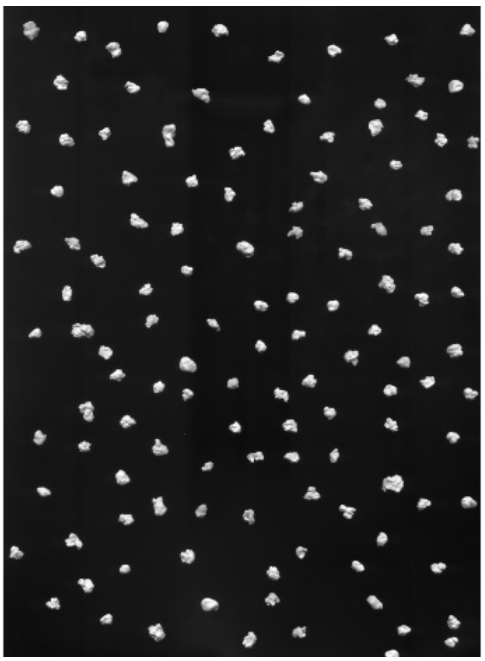

Figure 3.11: *MCC grains used during the tests.*

Using Image Tools it is possible to obtain the characteristic size properties of every particle. The software can recognise some very small particles which do not belong to the grains; so an initial screen of the data is needed, it is easy because the particles have been already sieved so we know the size range we are analyzing. Finally characteristic size properties of all the particles are collected and the mean is calculated.

Particles sphericity is assumed to be equal to their circularity and it is

Property	0.45 cm MCC Grains
Surface Area	$30.43[mm^2]$
Perimeter	$23.15[mm]$
Circularity	0.715

Table 3.6: *Image analysis results.*

calculated as:

$$\Phi_c = \frac{2\sqrt{\pi A}}{p} \simeq \Phi_s \tag{3.8}$$

where A is the surface area and p is the perimeter of the MCC grains.

The results of the Feret diameter, surface area are summarized in table 3.6

3.6 Shear Rate

The shear rate is the rate at which a progressive shear deformation is applied to some material. Consider the figure 3.12 where two parallel planes are separated by a height h: the lower plane stands still and the upper plane moves in the direction of the velocity v; the shear rate can be calculate as:

$$\dot{\gamma} = \frac{v}{h} \tag{3.9}$$

Figure 3.12: *Shear rate definition.*

The peculiarity of the simple shear apparatus is that the shear box is kept constant in every point so h is the bed height and v is obtained as the ratio of the displacement of the mobile wall in the x direction ϵ_x and the motion frequency which is kept constant in each test; so it can be calculated

using the expression 3.10.

$$\dot{\gamma} = \frac{\epsilon_x N}{ht} \tag{3.10}$$

where N is the number of cycles of the shear box, calculated as:

$$N = \frac{tf}{60} \tag{3.11}$$

t is the average time the percolate particle spends to move through the bed and f is the motion frequency of the mobile walls in the x axis.

3.7 Percolation Velocity

After several tests (typically 6-8) it is possible to calculate the average on the times of percolation for each case analyzed. The data have been divided in two categories: the particles which are placed close to the front and the back fixed walls and the particles which are placed in the center. Indeed the particles closer to the walls seem to be affected by a near-walls-effect.

The percolation velocity is defined as:

$$u_p = \frac{h}{t} \tag{3.12}$$

t is the average time the percolating particle spends to move through the bed and h is the bed height.

The percolation velocity can be normalized as:

$$U_p = \frac{u_p}{\dot{\gamma} d_B} \tag{3.13}$$

where d_B is the diameter of the bed particles and $\dot{\gamma}$ is the shear rate. This dimensionless group has been defined by Bridgwater in its articles. These physical quantities have different effect on the percolation speed.

3.8 Inertial Number

The shear rate can be normalized using the definition of the intertial number; which is defined as the ratio between the characteristic deformation timescale t_P and the characteristic confinement timescale t_γ. It can be expressed as:

$$I = \frac{t_P}{t_\gamma} \tag{3.14}$$

where the characteristic confinement timescale and deformation timescale are respectively the equations 3.15 and 3.16.

$$t_\gamma = \frac{1}{\dot{\gamma}} \tag{3.15}$$

$$t_P = d\sqrt{\frac{\rho}{P}} \tag{3.16}$$

Referring to the picture 3.13 the time t_γ is the macroscopic time needed for one layer to travel over a distance d with respect to an other; while t_P is the time needed by the top layer to be pushed back to its lower postion, once it has climbed over the next particle.

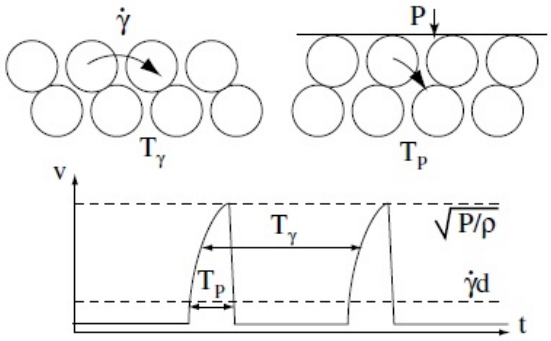

Figure 3.13: *Scheme of the physical meaning of the deformation timescale and the confinement timescale.*

Substituting the equations 3.16 and 3.15 in the equations 3.14 it is possible to obtain the inertial number expression:

$$I = \frac{\dot{\gamma}d}{\sqrt{\frac{P}{\rho}}} \tag{3.17}$$

The normal stress and the characteristic diameter need to be expressed for the simple shear apparatus system. The normal stress can be defined in three different ways, so three inertial numbers can be obtained:

1. Supposing that the pressure vary linearly and the height of one layer of the bed particles corresponds to the particle diameter d, the normal stress P can be written as:

$$P_1 = \rho g d_B \tag{3.18}$$

Considering the bed particle diameter and the normal stress P_1 the inertial number is:

$$I_1 = \frac{\dot{\gamma}}{\sqrt{\frac{g}{d_B}}} \tag{3.19}$$

2. The normal stress can be referred to the fine particle so P is obtained as:

$$P_2 = \rho g d_p \tag{3.20}$$

where d_p is the diameter of the fine particles. In this case the inertial number is expressed as:

$$I_2 = \frac{\gamma \dot{d}_B}{\sqrt{g d_p}} \tag{3.21}$$

3. Finally the normal stress can be defined using its general definition: force per unit of area. Considering the volume and the surface of a sphere it can be expressed as:

$$P_2 = \frac{m}{S} = \frac{\rho V}{S} = \rho \frac{\frac{\pi}{6} d_p^3 g}{\frac{\pi}{4} d_p^2} = \frac{2}{3} \rho g d_p \tag{3.22}$$

So the definition of the inertial number will be:

$$I_3 = \sqrt{\frac{3}{2}} \frac{\gamma \dot{d}_B}{\sqrt{g d_p}} \tag{3.23}$$

3.9 Diffusion Coefficient Calculation

The diffusion of the percolating particles is calculated using a Matlab code which compares different photograms to get the results. It uses four main steps:

1. A photogram of the top of the shear box is loaded. It shows the initial position of the particle on the top of the cell before beginning the test. They have the same position in every test. The domain which interests the analysis is smaller than the entire picture so it is possible to cut "the exceeding part" and select the domain which will be analyzed. Then the photogram is scaled using a one centimeter mark which is

drawn on the front wall of the box. So a scale factor (3.24) which is used to convert the measurament from pixel to centimeter is defined.

$$K_(px, cm) = \frac{Pixel}{Cm} \tag{3.24}$$

2. The pictures which show the bottom of the cell in the end of the test are cut and the dimensions of each photogram is adjusted to the top picture dimensions so that all the photograms are sized with the same dimensions and it is possible to compare them.

3. The particles which percolate are colored using three different colors: red, green and blue. They are selected in their position for each photogram analyzed respectively at the beginning and at the end of the test and their position is saved. The displacement on the x and y axes is calculated for each couple of photograms and the average value is calculated. In the end the code calculates the distance. In the figure 3.14 is shown a couple of photograms where the desired domain is selected and is used to calculate the displacements from the particles positions.

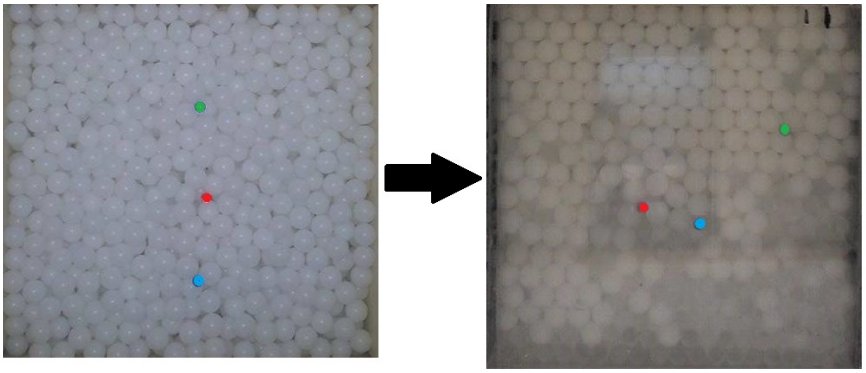

Figure 3.14: *Photograms of the top and bottom of the shear box respectively at the beginning and at the end of the tests* .

4. Finally it is possible to calculate the diffusion coefficient through the equations (4.9) and (3.26). It has two components respectively on the

x and the y directions.

$$D_x = \frac{\Delta x^2}{\Delta t} \tag{3.25}$$

$$D_y = \frac{\Delta y^2}{\Delta t} \tag{3.26}$$

where Δx and Δy are respectively the mean displacements in the x and the y directions and Δt is the average percolation time.

Chapter 4

Results and discussion

4.1 Introduction

In this chapter the results of data obtained using the simple shear box are shown and analyzed. In the first paragraph the percolation velocity of the spherical and granulated particles are described. The MCC grains have different shape and static friction coefficient so their behavior is more complex and their path through the bed is different. Then results on the diffusion coefficient, defined in the previous chapter, are discussed. Finally taking into consideration the experimantal results a model to describe the velocity percolation of the spherical particle will be shown.

4.2 Percolation velocity

In this section the particle percolation speed results are shown. At first the raw data are analyzed: it is explained the effects shear rate and the bed particles diameter have on percolation. Then to have a comparsion with the literature data the percolation speed has been normalized, using the Bridgwater dimensionless group.

The percolation velocities of the spheres and MCC grains are analyzed separately because of their own characterstic properties and then compared; so the effect of shape and friction coefficient can be shown.

All data have been measured using the second method, explained in the previous chapter. Indeed because of the simple shear box construction characteristic, it exists a zone of the cell which is affected by an undesired surface recirculation of the particles, which can slow down the percolation process of the fines. The goal of using the simple shear box in this thesis is to study percolation under controlled conditions so the method 2 has been chosen to get all the percolation speed measurement.

4.2.1 Spherical Particles

Two different beds made of spherical particles have been used during the tests. They have two different diameter sizes respectively 0.5 and 0.6 cm; so that the effect of the particles diameter is shown.

As it has been shown in the previous chapter, they have a very low coefficient of static friction; since in the industrial operations granular material have shapes which can be very different from a sphere; the effect of the shape on the percolation velocity will be studied in a dedicated section.

Raw Data

In the figure 4.1 it is shown how the percolation speed u_p varies with the diameter ratio between the fine and coarser particles d_p/d_B . This curves are obtained using a glass 0.5 cm diameter particle bed.

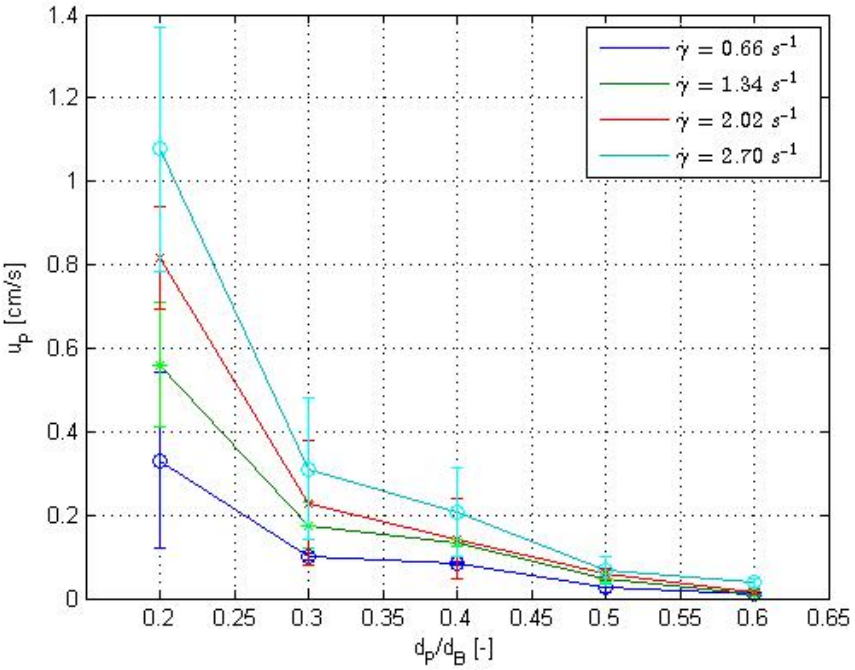

Figure 4.1: *Plot of Percolation Velocity of the spherical particles versus the diameter ratio of the spherical particles; using a bed with a diameter particle of a 0.5 cm.*

The velocity decreases when the diameter ratio is increased. When fine particle size increases they cannot find easily free spaces through which they can flow. Consequently the percolation time increases. This behavior has

been estimated by Bridgwater who found the following relationship to express the percolation velocity:

$$\frac{u_p}{\dot{\gamma} d_B} = k_g e^{-k_s d_p / k_r d_B} \tag{4.1}$$

where k_g, k_s and k_r are constat values.

A simple expression which can be used to describe the average space between particle in packed bed for spherical particles is:

$$\bar{h} = \frac{2}{3} d_B \frac{\epsilon}{1-\epsilon} \tag{4.2}$$

where ϵ is the bed porosity. So the percolating particles must have a size smaller than $\bar{h}$ otherwise they cannot pass through the bed.

In figure 4.1 it is possible to see that when the size diameter ratio is very low (e.g. for d_p/d_B equal to 0.2) the errorbars are larger. Indeed during the tests, performed using the simple shear box, it has been seen that if the fine particle are small enough and if they are in the proximity of some voids, due to the bed particles arrangement, fines can directly fall through the voids and significantly reduce their path (*Spontaneous Percolation*). It can affect the measurement because it begins after the simple shear cell is completely filled so there is a higher variability in the collected data.

When the shear rate increased, the percolation speed presented higher values; indeed at higher shear rate the bed particles can re-arrange themself faster and the fine particles are exposed with a large frequency to voids, so they can pass through the bed faster.

To better see the exponential behavior of the percolation velocity, which was already established by Bridgwater (see equation 4.1), the logarithm of the percolation velocity is plotted against the diameter ratio and a linear regression has been performed. In table 4.1 are summarized the results.

$\dot{\gamma}$	m	q	R^2
0.67	-8.6	0.58	0.9825
1.35	-9.1	1.3	0.981
2.02	-9.3	1.6	0.989
2.70	-8.2	1.6	0.990

Table 4.1: *Linear regression results of the Percolation velocity versus the diameter ratio.*

The determination coefficients R^2 are all close to the 0.99 so that the lines represent the data in the good way and the exponential behavior of the percolation velocity has been definitely proved.

Finally a comparison between the linear regression and the raw data are plotted in the figure 4.2.

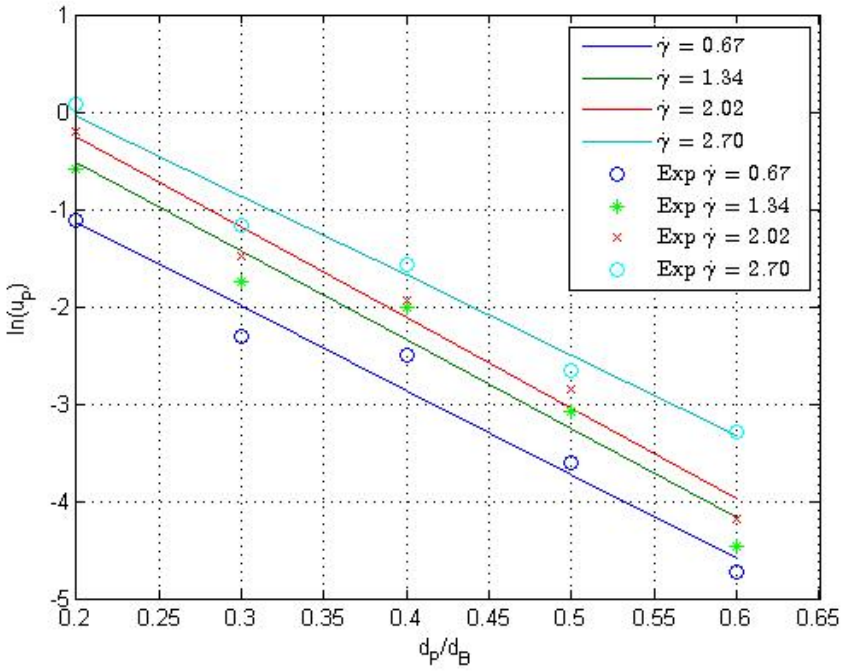

Figure 4.2: *Plot of percolation velocity logarithm versus the diameter ratio of the spherical particles. The linear regression are compared with the experimental data. The diameter particle bed is equal to 0.5 cm.*

Shear Rate Effect

The simple shear box permits to change the intensity of the shear rate on the testing materials, by changing the motion frequency of the lateral walls. In percolation a higher shear rate applied to the bed could be considered as a faster rearrangement of all the particle layers present in the bed, giving the possibility to the fine particles to be exposed at new voids and go on in their path.

During the tests, four different shear rates have been chosen to asses the percolation velocity dependency; they are respectively: 0.67, 1.35, 2.02, 2.70 s^{-1} . Figure 4.3 shows the percolation velocity plotted as a function of the shear rate $\dot{\gamma}$. The curves are parametric for each diameter ratio.

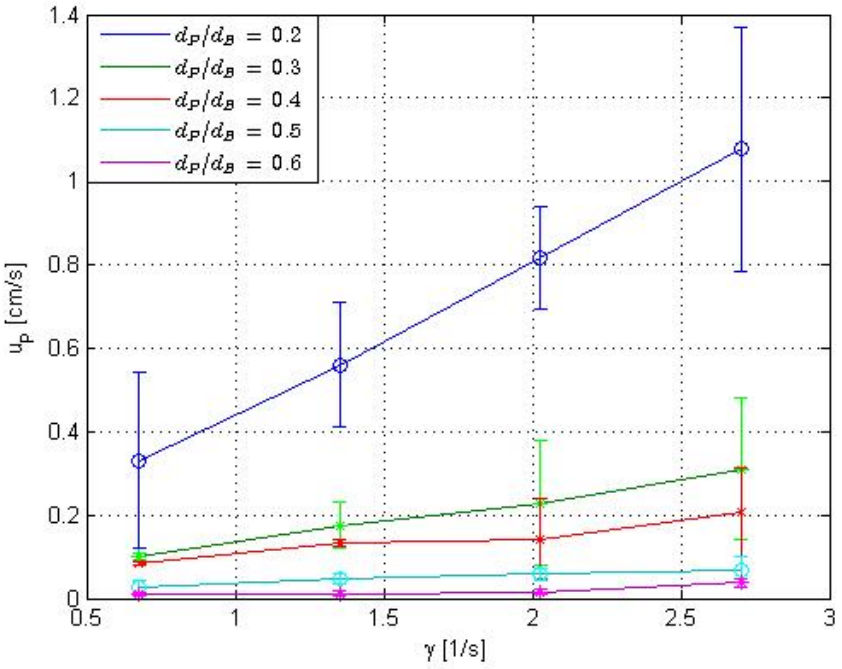

Figure 4.3: *Plot of Percolation Velocity versus the shear rate of the spherical particles using a bed with a diameter particle of a 0.5 cm.*

From this graph it is clear that the percolation velocity has a linear dependency on the shear rate.

To demonstrate the linearity of this relationship, linear regressions have been calculated for each curve. The results of all the regressions are summarized in the table 4.2.

d_p/d_B	m	q	R^2
0.2	0.37	0.073	0.998
0.3	0.081	0.033	0.992
0.4	0.057	0.046	0.935
0.5	0.021	0.015	0.982
0.6	0.013	0.0041	0.789

Table 4.2: *Percolation velocity regression results.*

Here it is possble to see that the intercept values are very close to zero: it corresponds to a state where there is not shear rate so that the fine particles can flow only if they find free space in the bed, otherwise they just stop. This particular situation has been defined as *Spontaneous Percolation*; so

the particles can fall through all the bed height only if they are small enough and do not find any obstacles.

Since in the experiments was never observed, it has been decided to consider a situation which does not involve a spontaneous percolation; so new linear regressions have been calculated, forcing all the curves to pass to the axes origin. The results of the new regressions are shown in the table 4.3.

d_p/d_B	m	R^2
0.2	0.405	0.998
0.3	0.117	0.991
0.4	0.079	0.935
0.5	0.028	0.984
0.6	0.011	0.785

Table 4.3: *Percolation velocity regression results forcing the intercept to zero.*

Comparing the tables 4.2 and 4.3 it can be observed that the determination coefficients do not vary significantly, while the slopes of the curves increase; furthermore they are inversely proportional with the diameter size ratio.

To study this dependency slope of the regression lines were plotted against the diameter ratio and fitted using different expressions. Data were fitted using an exponential and a polynomial models, where non linear least squares methods have been used.

An exponential model describes fine particles speed as:

$$u_p = Ae^{(B\frac{d_p}{d_B})}|\dot{\gamma}| \tag{4.3}$$

This model has been chosen considering the previous experimental results (see 4.1); furthermore the exponential behavior of particles percolation velocity has been already proved experimentally and theoretically, using the statistical mechanics, by Bridgwater (1985).

Morever considering the expression of the flux segregation appeared in the model developed by Santomaso and co-workers (2015):

$$u_p = -Kd_B(1-\omega_f)(\frac{d_p}{d_B}-1)|\dot{\gamma}|^m \tag{4.4}$$

where K is a model parameter d_p and d_B are respectively the diameters of the fine and coarse particles, $\dot{\gamma}$ is the value of the shear rate and ω_f is the fines concentration. Morever the system is very diluited the fines concentration is

zero; so the equation 4.4 becomes:

$$u_p = -Kd_B(\frac{d_p}{d_B} - 1)|\dot{\gamma}|^m \tag{4.5}$$

The linear dipendency of the shear rate in the analyzed range, from 0.67 to 2.70 s^{-1}, has been shown above; to understand the diameter size ratio dependency using the equation 4.4; so the exponent m is set to one.

The polynomial model which considers equation 4.5 is:

$$u_p = A(1 - \frac{d_p}{d_B})^N|\dot{\gamma}| \tag{4.6}$$

In figure 4.4 is shown the curves which have been used to fit the data compared with percolation velocity slopes. In all cases it has been decided to simulate a case which the spontaneous percolation is not involved.

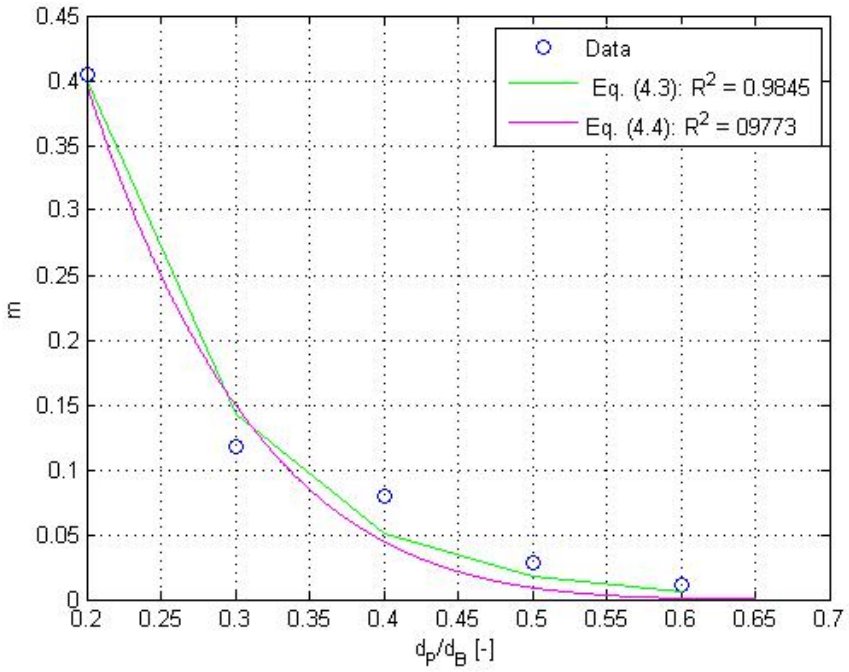

Figure 4.4: *Fitting of the angular coefficients of the shear rate line for the spherical particles.*

The results of the model coefficients, determination coefficients R^2 of the different models are summarized in the table 4.4.

Model	Coefficients			R^2
	A	B	N	
$Ae^{(B\frac{d_p}{d_B})}\|\dot{\gamma}\|$	3.162	-10.33		0.9845
$A(1-\frac{d_p}{d_B})^N\|\dot{\gamma}\|$	2.157		7.56	0.9773

Table 4.4: *Percolation velocity regression results.*

Even though the model 4.6, refered to 4.4 gives good resullts, the exponential model is better.

Particle Bed Diameter Effect

All the data reported above have been obtained using the same bed, made of 0.5 cm glass spherical particles. To study the effect of the bed particle diameter on the percolation speed, few tests have been performed in a limited diameter ratio range, from 0.3 to 0.5 cm. The height of the bed from the percolation velocity of fines has been measured is the same.

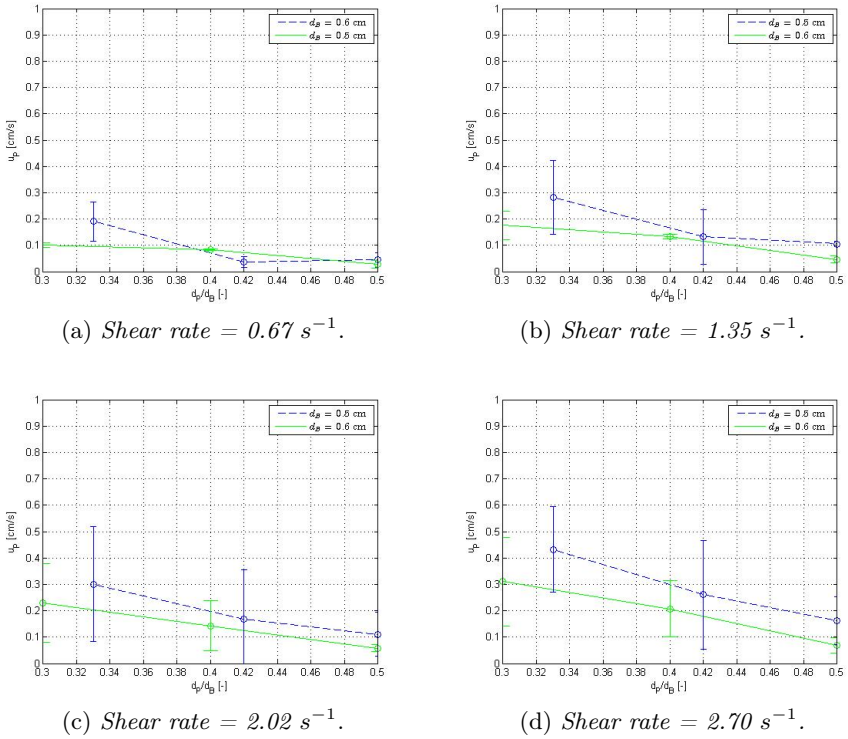

(a) *Shear rate = 0.67* s^{-1}.

(b) *Shear rate = 1.35* s^{-1}.

(c) *Shear rate = 2.02* s^{-1}.

(d) *Shear rate = 2.70* s^{-1}.

Figure 4.5: *Comparsion of the percolation velocity of the spherical particles using two different bed diameter particle sizes: respectively 0.5 and 0.6 cm .*

The effect is shown in the figure 4.5, where every graph represents a certain velocity obtained at a specific shear rate.

At every shear rate fine percolation velocity increases when the bed particles diameter is higher. The porosity of the two beds are basically the same, as it has been shown in the previous chapter; so because the height if the beds was kept constant, the difference between the two curves depend on the fact that fine particles when fall through the beds cross a smaller number of particles layers and the free height is larger.

However only a small range of the size ratio have been investigated; furthermore the sizes of the bed diameter particles is very close: they differ in size for only 1 mm, so a deeper study is needed.

Dimensionless Speed

All the results considered up to now are based on their characteristic dimensions; to have a comparison with the literature data, dimensionless physical quantities are required.

In figure 4.6 it is shown a comparison of the data obtained during this experimental work with the Bridgwater results.

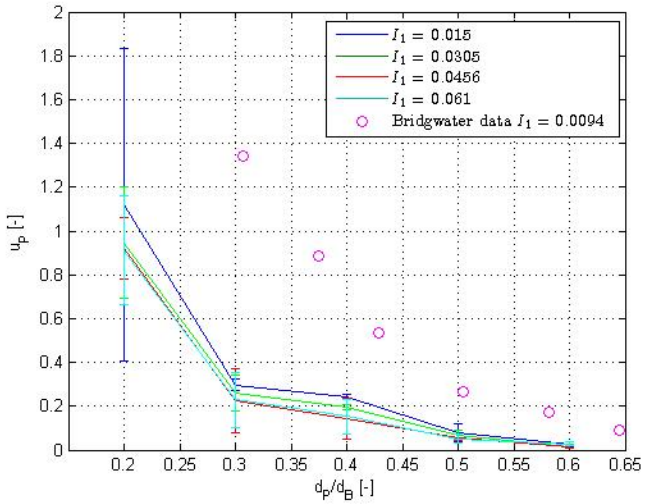

Figure 4.6: *Plot of Percolation Velocity of the spherical particles versus the diameter ratio of the spherical particles; using a bed with a diameter particle of a 0.5 cm.*

As Bridgwater suggested, the percolation velocity can be normalized as:

$$U_p = \frac{u_p}{\dot{\gamma} d_B} \tag{4.7}$$

I_1 is the dimensionless shear rate, which has been expressed using the inertial number 4.8.

$$I_1 = \frac{\dot{\gamma}}{\sqrt{\frac{g}{d_B}}} \tag{4.8}$$

The colored lines represents the percolation velocities at different shear rates normalized using the equation 4.7, which have been measured using a bed made of 0.5 cm size diameter spheres, while the red dots are the Bridgwater data (1985).

The trends of the data are the same: they both deacrease exponentially when the size ratio increases, but the values of the percolation velocity are significantly lower than Bridgwater results.

It is due to the fact that in his experiment Bridgwater used a 2.45 cm size diameter glass spheres, which is very high compared to the size diameter used in the new performed tests. Indeed, as it was shown in the previous section, the absolute diameter of bed particles can influence the percolation speed.

4.2.2 Irregular Particles

This section shows the results of the percolation velocity for the MCC grains which were analyzed using the simple shear box. The grains differ from the sphere for the shape and coefficient of friction. The shape has been evaluated using image analysis and it is equal to 0.71; while the friction coefficients are significantly higher. Morever grainulated particles can be used to describe an industrial application in a more accurate way.

Two different diameter bed sizes have been used during these tests, respectively 0.38 and 0.45 cm. The diameter ratios are obtained varying the percolating particles; furthermore four different shear rates have been used to investigate their effect on the percolation velocity.

As in the previous section at first the raw data are shown and then dimensioless speed curves are illustrated.

Raw Data

Figure 4.7 shows how the grains percolation velocity u_p varies with the diameter ratio d_p/d_B. To calculate the diameter ratio an average sieve diameter has been considered. All data have been measured using a bed made of 0.45 cm size diameter MCC grains.

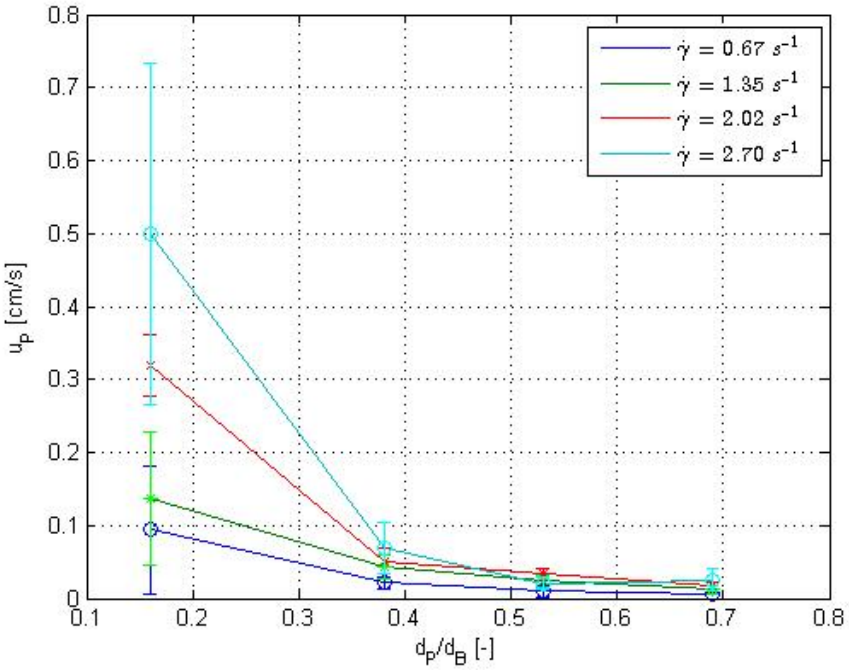

Figure 4.7: *Plot of Percolation Velocity versus the diameter ratio of the granulated particles using a bed with a mean diameter particle of a 0.45 cm.*

From the graph above it is possible to see that the percolation speed becomes slower when the size ratio d_p/d_B increases. Decreasing the shear rate they decrease exponentially. The speed tends to zero very soon when the fine grains size is increased; because of the particles shape their path could be very tortuous.

The percolation velocity of grains presents a very high standard deviation compared to the measurement for spheres; due to the initial spontaneous percolation the fines could occur in the bed before the measurement begins.

The shear rate influences the percolation time so when the bed rearranges itself faster, new voids, which permits the fine particles to move into the bed, are generated.

Linear regressions have been calculated for the logarithm of the percolation velocity against the diameter ratio d_p/d_B. Table 4.5 summarizes the results.

$\dot{\gamma}$	m	q	R^2
0.67	-5.1	1.7	0.9525
1.35	-4.6	1.3	0.996
2.02	-5.5	0.5	0.974
2.70	-6	-0.1	0.925

Table 4.5: *Linear regression results of the Percolation velocity versus the diameter ratio.*

Comparing these results to the outcome obtained analyzing the spherical particles (see table 4.1) it is possible to see that the determination coefficients are lower but they are very close to the unity; hence the grains behavior can be described using an exponential law.

Shear Rate Effect

Figure 4.8 shows how the percolation velocity increases when the shear rate increased.

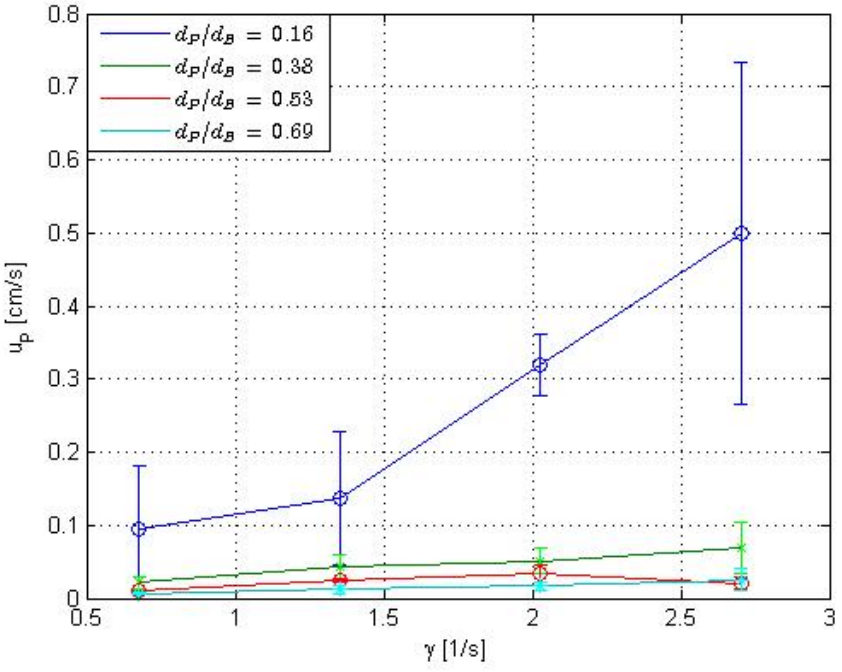

Figure 4.8: *Plot of Percolation velocity versus the shear rate of the granulated particles using a bed with a mean diameter particle of a 0.45 cm.*

In the graph the shear rate seems to have an higher effect on the finest particles speed. However the dependency is barely linear; so the data have been modeled with a straight line.

During the fines speed measurement four different shear rates have been set and kept constant, controlling walls motion of the simple shear box, respectively: 0.67, 1.35, 2.02, 2.70 s^{-1}.

To see the grains behavior a linear regression has been calculated for each curve. In the table 4.6 the results are reported.

d_p/d_B	m	q	R^2
0.16	0.41	0.088	0.943
0.38	0.045	0.008	0.971
0.53	0.013	0.011	0.566
0.69	0.018	8.2x10^{-5}	0.974

Table 4.6: *Percolation velocity regression results.*

The intercepts values are very close to zero so that the spontaneous percolation seems to be reduced, unless than at a diameter ratio d_p/d_B of 0.16 cm which presents a very low value; the high standard deviation of the curve is an additional index that spontaneous percolation it can easily occur.

The reason of this low values is probabily the low frictional coefficients of the MCC grains.

The curves slopes decrease rapidly when the fine particle size increases.

The data at a d_p/d_B of 0.53 have a very low determination coefficient, it can represent an experimental mistake.

To simulate a situation where spontaneous percolation is completly absent, new linear regressions have been calcuted into curves intercepts are forced to pass to zero and the new results are reported in the table 4.7.

d_p/d_B	m	R^2
0.16	0.164	0.971
0.38	0.026	0.986
0.53	0.012	0.566
0.69	0.009	0.986

Table 4.7: *Percolation Velocity Regression Results forcing the intercept to zero.*

The determination coefficients R^2 increase significantly compared to the previous case (see table 4.6). When d_p/d_B is equal to 0.53 the determination coefficient is still very low, so there could be an experimental error.

From the second column of table 4.7 values obtained from the linear regressions is possible to see, when the diameter particle ratio increases the slopes m decreases significantely.

Considering the analyzed shear rate range, the trend of the slopes percolation velocity curves has been studied in depth.

Data have been fitted using the models 4.3 and 4.6. The models do not consider the spontaneous percolation contribute, which, in this case, seems to do not affect the measurement. Non linear least squares methods has been used to solve fittings.

Figure 4.9 represents the slopes values against the size ratio, as dots, and their respectively fitting.

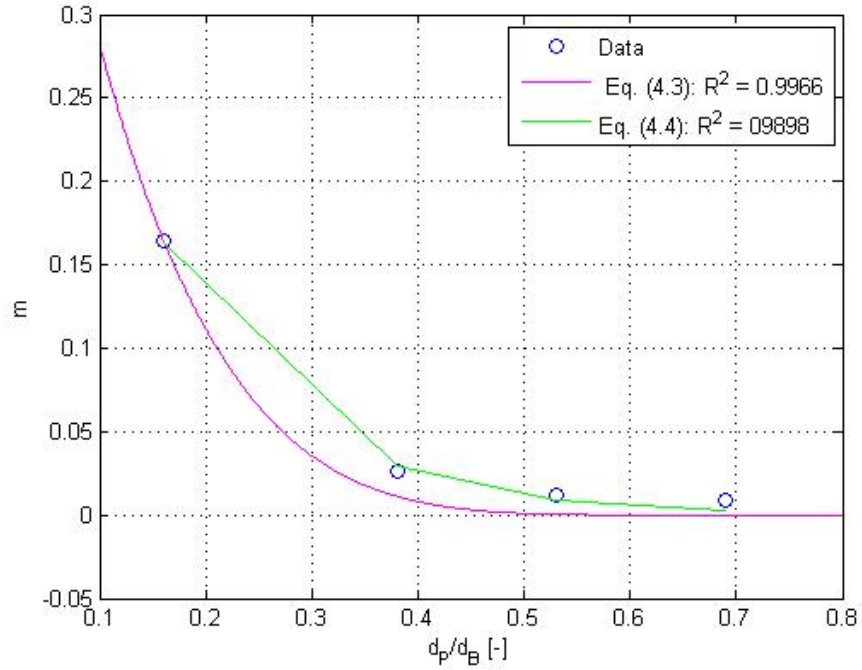

Figure 4.9: *Fitting of the angular coefficients of the shear rate line for the grains.*

Finally table 4.8 shows the results of the determination coefficients and models parameters for the different fitting attempted, which are shown in figure 4.9.

Model	Coefficients			R^2
	A	B	N	
$Ae^{(B\frac{d_p}{d_B})}\|\dot{\gamma}\|$	0.5724	-7.818		0.9966
$A(1-\frac{d_p}{d_B})^N\|\dot{\gamma}\|$	0.4398		5.66	0.9898

Table 4.8: *Percolation Velocity Regression Results.*

Observing the curves determination coefficients R^2 it is possible to see that the exponential regression fit the data better than the polynomial.

Dimensionless Speed

In this section the percolation speed of the grains has been normalized, as Bridgwater suggested (1985), using the expression 4.7. The results are shown in figure 4.10.

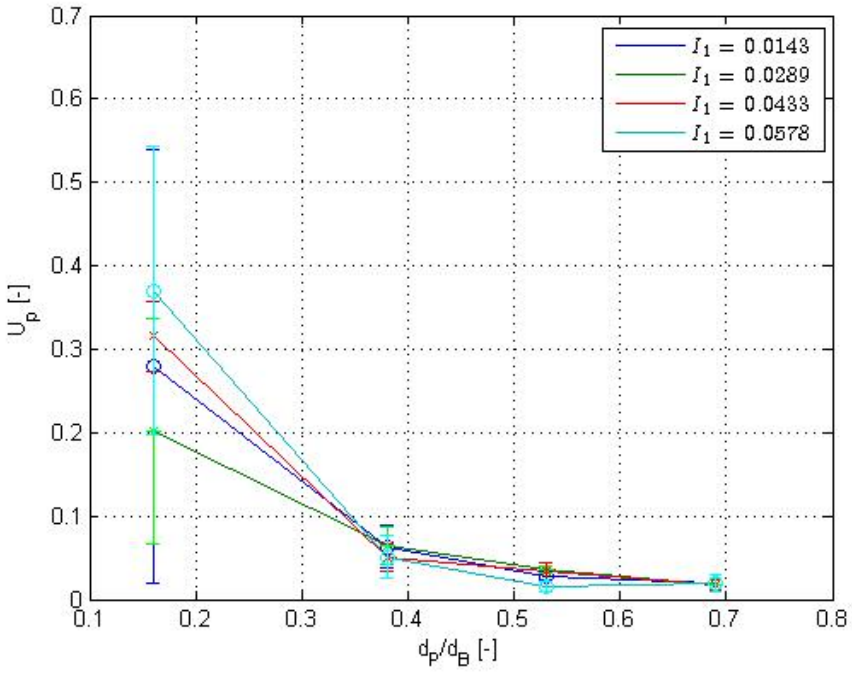

Figure 4.10: *Plot of the dimensionless percolation velocity versus the diameter ratio for grains.*

Again particle velocities collapse into the same curve so it is possible to see that they decrease when the diameter ratio increases.

4.2.3 Comparison of the percolation velocities

The percolation velocity of two different granular materials have been investigated separately in the above paragraphs. In this section a comparison between their percolation velocity is made. Figures 4.11 and 4.12 show the velocity of the spheres and the grains; every graph refers to the percolation speed measured at the same shear rate.

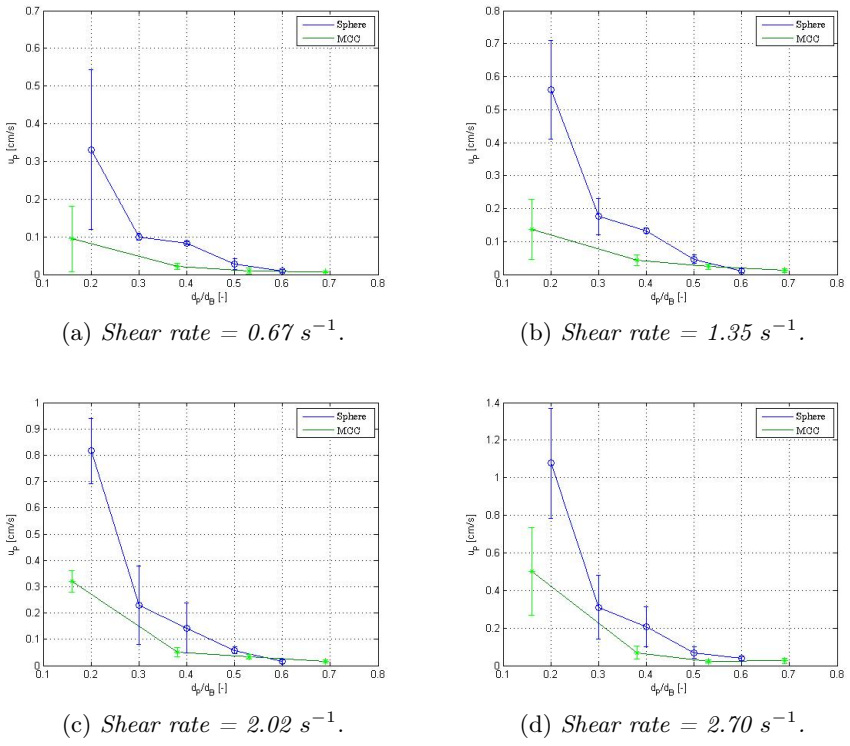

(a) *Shear rate = 0.67* s^{-1}. (b) *Shear rate = 1.35* s^{-1}.

(c) *Shear rate = 2.02* s^{-1}. (d) *Shear rate = 2.70* s^{-1}.

Figure 4.11: *Comparison of the percolation velocity of two different materials: glass and MCC particles* .

At every shear rate the spheres percolate faster than the grains. Indeed the grains have a higher coefficient of friction; furthermore they are not perfectly spherical so because of their shape the fine particle path could be hindered easily by a bed particles.

The speeds have been measured with two different bed sizes even if they are very close: they are respectively 0.5 cm for the glass spheres and 0.45 cm for the MCC grains. As it has been shown above the bed diameter size influences the percolation velocity so it also could contribute to increase the difference between the curves. Furthermore the grains diameter size is very difficult to evaluate because of the irregular shape so it has been considered a sieve diamter which differs from the real one.

While the spheres have an exponential trend, grains seems to have two different flow regimes. They show a change in slope around a diameter ratio d_p/d_b equal to 0.4.

This behavior is also shown comparing tables 4.2 and 4.5, in particular the determination coefficients of the grains are not very close to the unity as spherical particles.

Dimensionless Speed

The dimensionless percolation velocities of the spheres and grains are shown in figure 4.12. Every graph represents the comparison of two curves of different materials which have been obtained at the same shear. The percolation velocity has been calculated using the 4.7.

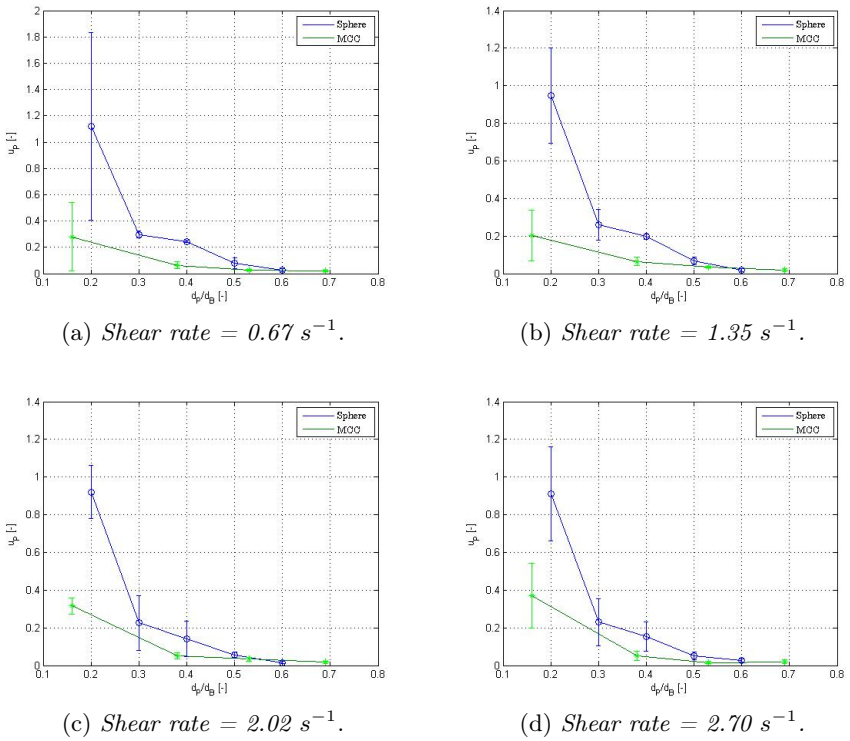

(a) *Shear rate = 0.67* s^{-1}.

(b) *Shear rate = 1.35* s^{-1}.

(c) *Shear rate = 2.02* s^{-1}.

(d) *Shear rate = 2.70* s^{-1}.

Figure 4.12: *Comparison of the percolation velocity of two different materials: glass and MCC particles normalized using the expression 4.7.*

The MCC particles percolate slower than the spheres in all the cases. Therefore an additional effect must exist due to the shape and the static frictional coefficient.

4.2.4 Different materials mixtures

More tests have been performed using mixtures of two different materials. In figure 4.13 the results of tests performed using MCC particles as fines and a bed of coarse made of glass spheres are shown.

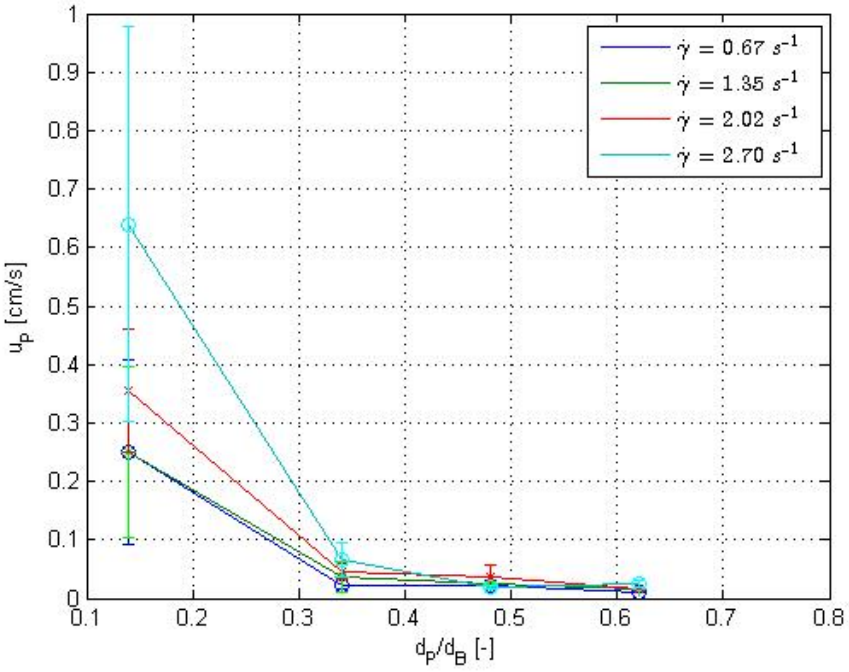

Figure 4.13: *Plot of Percolation velocity of the MCC particles versus the diameter ratio; using a bed made of glass spherical particles with a diameter of 0.5 cm.*

As it was shown above, also in this case percolation velocity decreases with the diameter ratios and it is proportional to the shear rate. In this graph the errorbars are significantly large, indeed it has been seen that there is a very high variabiliy in the recorded percolation times. The shape of the fine particles could affect the measuration, so that each particle can flow through the bed in different ways; this aspect needs to be investigated in depth.

4.3 Diffusion Coefficient

In this section the data measured on the diffusion coefficient are discussed. This analysis have been performed to see what happens to the fine

particles path when there is a change in the percolation velocity conditions. Indeed the ways they take to cross the bulk bed particles is always very mazy. The measurements have been performed using image analysis; the method has been explained in the previous chapter.

In figures 4.14 and 4.15 the results are shown, respectively for spherical and irregular particles. The graphs show how the components of the diffusion coefficient varies with the shear rate and diameter ratio, on the x and y axis of the simple shear box (see figure 3.1). In the equations 4.9 the diffusion coefficient components are defined.

$$D_x = \frac{\Delta x^2}{\Delta t}; D_y = \frac{\Delta y^2}{\Delta t} \tag{4.9}$$

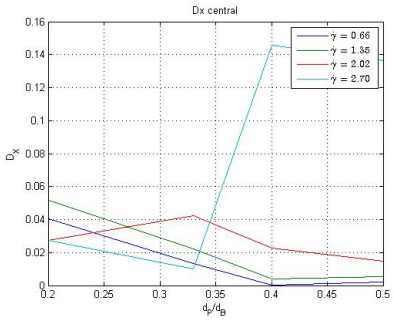

(a) *X Diffusion Coefficient Component versus the ratio diameter.*

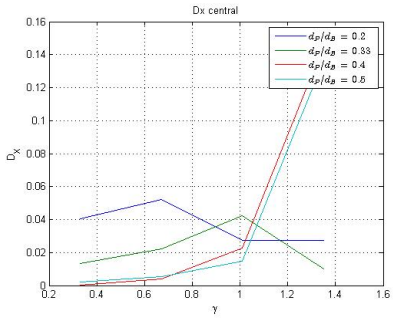

(b) *X Diffusion Coefficient Component versus the shear rate.*

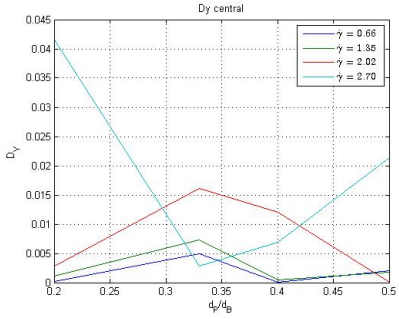

(c) *Y Diffusion Coefficient Component versus the ratio diameter.*

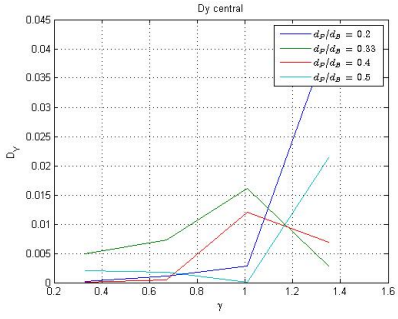

(d) *Y Diffusion Coefficient Component versus the shear rate.*

Figure 4.14: *Diffusion coefficient components of the spherical particles.*

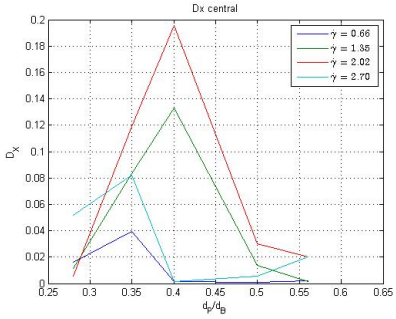

(a) *X Diffusion Coefficient Component versus the ratio diameter.*

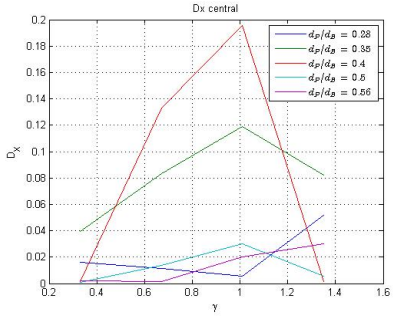

(b) *X Diffusion Coefficient Component versus the shear rate.*

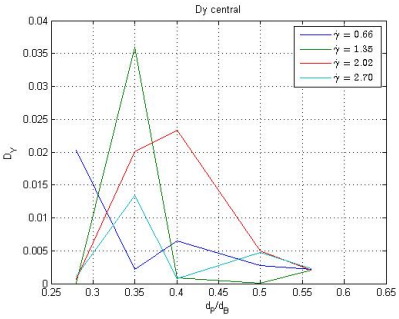

(c) *Y Diffusion Coefficient Component versus the ratio diameter.*

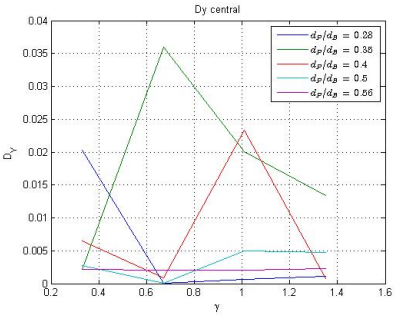

(d) *Y Diffusion Coefficient Component versus the shear rate.*

Figure 4.15: *Diffusion coefficient components of the MCC particles.*

The particles do not show to have a preferential path at every variations: it has been investigated the difference in sizes, shapes and shear rates. Their motions across the bed on the x and y axis (considering the simple shear apparatus axes definitions) seem to be totally random. Their path depends on the probability of finding a free space on the bed to fall down. The problem is to take a measure of the avalability of voids inside the bed in every position and in every moment can be very difficult and performed only using a direct measurement methods; otherwise a DEM simulation analysis is required.

Furthermore it has to be said that these analysis was not investigated in depth; indeed it was performed only using the first measurement method, presented in the previous chapter, so the measurements are affected to a certain disturb due to the recirculation of the particles on the bed surface. Also the bias effect of the bed diameter sizes was still not considered, so the diameter ratios were obtained using two different beds in both cases. So a deeper analysis is required to asses this aspect.

4.4 Percolation velocity model

In this section a model to describe the percolation velocity is presented. It has been developed on the basis of the considerations made in the previous section about the percolation velocity and the literature knowledge.

As Bridgwater affirms the fine particles need three main conditions to percolate through a bed:

1. The fines must be small enough to fit through the matrix which is formed by the void between the coarse particle.
2. Inter-particle motion or a strain must exist to allow the opportunities for fines to be exposed to multiple voids.
3. Fines need to be significantly free-flowing to pass through the pores.

Hence when fine particles flow through a bed, during all their path they find many obstacles (typically a coarser particle); therefore the percolation can be described as an un-continuous phenomena. Specifically the percolation time can be considered as results of times when fine particles fall into the voids and times when particles are stopped by an obstacle; to create new free spaces they can fall into, an external stress is required, which in the simple shear box is given by the shear stress, applied by its lateral walls.

Notwithstanding its important role, Bridgwater (1994) did not consider bed porosity ϵ as an indipendent variable and did not include it in his theory. The voidage is strongly connected with the probability of fines to find free spaces they can pass through; so it needs to be included.

In the following sections the model is described in detail and the results are compared with the experimental data.

4.4.1 Model

Average distance between bulk particles

The voidage of the bulk material is an important variable which characterize the average distance between the coarse particles. It has been shown above that for spherical particles in random packaging can be expressed through the equation 4.2. Considering that the bed porosity measured during experimental tests was equal to 0.4, it is possible to evaluate the average distance $\bar{h}$ as:

$$\bar{h} = 0.44 d_B \tag{4.10}$$

Morever equation 4.2 has been assumed to be the average chord lenght betweeen two surface points of two spheres. Hence it works only for spherical particles.

Probability of passing for the fines

Considering figure 4.16, where a schematical cage made of three coarse particles delimited a fine particle.

A fine particle, if it is small enough and find a free space, can flow in the y direction because of gravity, and its path is $d_B - d_p$. While the motion of the coarse bed particles (in the x direction) is due to an external strain, the shear rate. The distance between the centers of two adjacent particles in the direction of the motion is $d_B + \bar{h}$

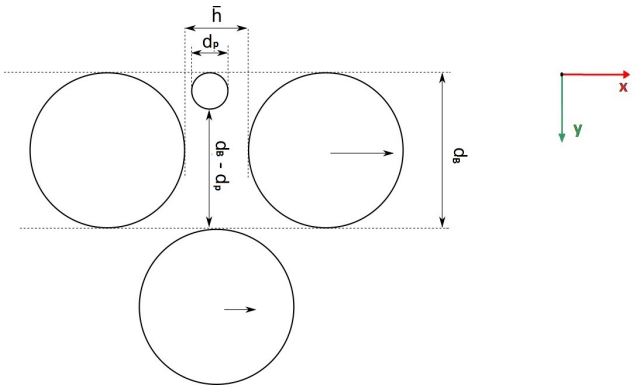

Figure 4.16: *Scheme of a cage where the coarse and fine particles are shown with their respectively characteristic lengths.*

Percolation velocity of fine particles depends on their probability to find free spaces they can fall through in a bed of coarser particle. As it has been shown above the average free space in a bed of spherical particle in a packed bed can be estimated using the 4.10. Cooke and Bridgwater(1979) demonstrated , using the statistical mechanical, that the probabiliy distribution of the distance between two particles is $P(h) = \frac{1}{\bar{h}} e^{-\frac{h}{\bar{h}}}$.

The probability to find a free space between h and $h + dh$ is :

$$P(h) = \frac{1}{\bar{h}} e^{-\frac{h}{\bar{h}}} dh \tag{4.11}$$

The fine particle diameter is d_p so their size must be smaller than the average distance between particles $\bar{h}$. Hence the probability to move across the bed can be calculated as:

$$P(h \geq d_p) = \int_{d_p}^{inf} \frac{1}{\bar{h}} e^{-\frac{h}{\bar{h}}} dh = e^{-\frac{d_p}{\bar{h}}} \tag{4.12}$$

Falling conditions for fines

Two limiting cases can be thought:

1. The free fall, which occurs when $\bar{h} > d_p$, during the flight so that the fine particle can move undisturbed in all the cage.

2. The hindered fall $\bar{h} = d_p$, which cover the case of multiple stops and go during the fall unit cage or shorter path.

The idea of this model is to split the percolation time 4.13 in two components a free fall time t_f, and a stop time t_s. The first depends on the probability that the fine particles have to find a free space in the bed they can pass through,which can be expressed by the 4.12; while the second is time the particle is stopped by the bed particles before it finds an aperture.

$$t_{tot} = Pt_f + (1 - P)t_s \tag{4.13}$$

The free fall time is proportional to the difference between the coarse and the fine particles, as shown in the figure 4.16, and varies inversely with the velocity the fine particle takes in his falling step.

$$t_f \propto \frac{(d_B - d_p)}{u_f} \tag{4.14}$$

An average velocity can be estimated through an energy balance considering that the potential and kinetic energies:

$$\Delta E_k + \Delta E_p = 0 \tag{4.15}$$

Energy balance terms are explicited so the 4.15 becames:

$$\frac{1}{2}\rho u_f^2 = \rho g(d_B - d_p) \tag{4.16}$$

Hence the velocity u_f is found.

$$u_f \propto \sqrt{g(d_B - d_p)} \tag{4.17}$$

Finally, substituting the velocity into the 4.14 t_f, can be calculated as:

$$t_f \propto \sqrt{\frac{(d_B - d_p)}{g}} \tag{4.18}$$

The stop time t_s occurs when fines are not allowed to move because they are hindered by an obstacle, to make them fall in the next step an external stress is required to change the bed particles disposition and create new voids they can fall through. It can be expressed as:

$$t_s \propto \frac{(d_B + d_p)}{u_c} \tag{4.19}$$

where u_c is the time of the re-arrangement of the bed particles due to the shear rate $\dot{\gamma}$.

$$u_c = \dot{\gamma} d_B \tag{4.20}$$

Substituting u_c in the 4.19 the stop time can be calculated as:

$$t_s \propto \frac{d_B + d_p}{\dot{\gamma} d_B} \tag{4.21}$$

Percolation velocity

Percolation velocity is proportional to the difference between the coarse and the fine particles and total inversely of percolation time.

$$u_p \propto \frac{d_B - d_p}{t_{tot}} \tag{4.22}$$

Substituting the 4.13 in the percolation velocity equation and expliciting all the terms, after some manipulation 4.22 can be written as:

$$u_p \propto \frac{d_B(1 - \frac{d_p}{d_B})\dot{\gamma}}{(1 + \frac{d_p}{d_B})(1 - P) + \dot{\gamma}\sqrt{\frac{d_B - d_p}{g}}\sqrt{1 - \frac{d_p}{d_B}}P} \tag{4.23}$$

The dimensionless percolation velocity can be expressed as:

$$U_p \propto \frac{1 - d^*}{(1 + d^*)(1 - P) + \dot{\gamma}^*(1 - d^*)^{0.5}P} \tag{4.24}$$

where:

$$U_p = \frac{u_p}{\dot{\gamma} d_B}; \dot{\gamma}^* = \frac{\dot{\gamma}}{\sqrt{\frac{g}{d_B}}}; d^* = \frac{d_p}{d_B} \tag{4.25}$$

The hindered fall

For higher size ratio the percolation process does not involve through free falls but hindered ones. Indeed at $\bar{h} = d_p$ it can be found a limit ($d_p/d_B = 0.44$) above which the percolation particles trajectory is strongly affected by the coarse particles of the cage. Furthermore the distance $d_B - d_p$ becomes smaller when the fine particle size increases.

From equation 4.24 when percolation velocity is zero when the size ratio $d_B/d_p = 1$; anyway experimentally has been found that at diameter ratio of 0.6 the velocity is very close to zero. A correction factor can be introduced to take in account the hindering effects of the cage of coarse particles when $d_B/d_p > 0.44$. The free fall distance can be reduced by a factor k as $d_B - kd_p$ where $k = 1.5$. This correction bears some analogies with the one used by

Beverloo to predict the mass flow rate of free falling particles through an orefice.

4.4.2 Experimental Data Comparison

In this section the model, explained above is compared with the experimental results obtained using the simple shear apparatus. Figures 4.17 and 4.18 show respectively the plots of percolation velocity versus the diameter ratio and the shear rate.

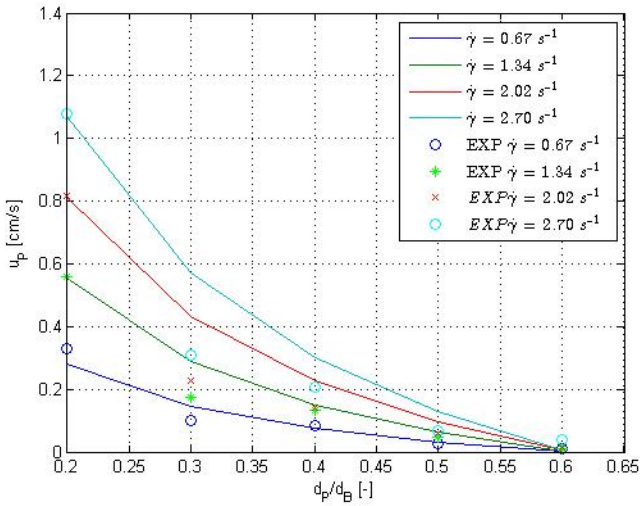

Figure 4.17: *Comparison of the percolation velocity model with the experiment data. The percolation speed is plotted versus the diameter size ratio.*

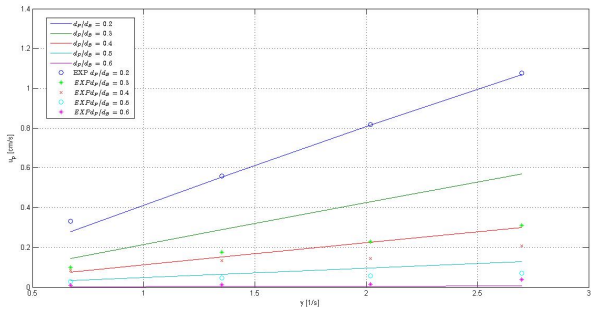

Figure 4.18: *Comparison of the Percolation velocity model with the experiment data. The percolation velocity is plotted versus the shear rate.*

The model predicts qualitatively but not quantitatively good the experimental data. So according to a fitting found from them, an exponent n is

added to the term $(1 - d^*)$. Therfore equation 4.25 becomes:

$$U_p = A\frac{(1 - kd^*)^n}{(1 + d^*)(1 - P) + \dot{\gamma}^*(1 - kd^*)^{0.5n}P} \tag{4.26}$$

where the parameters are $A = 2.6, k = 1.5$ and $n = 3$. In figure 4.19 the graphs of the dimensionless percolation velocity and the comparison with the experimental data.

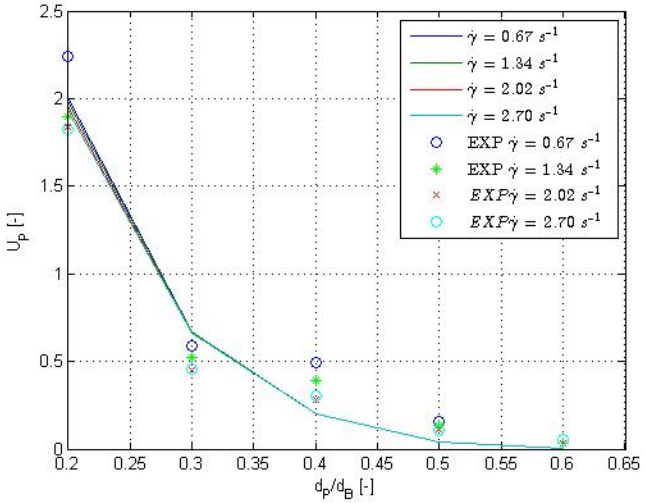

Figure 4.19: *Comparison of the dimensionless percolation velocity model with the experiment data. The percolation velocity is plotted versus the diameter ratio.*

As in the percolation speed experimental results, calculated dimensionless velocities collapse in one curve. Determinantion coefficients of every curves has been calculated to show the goodness of the model prediction. Results are summarized in table 4.9.

Model	Shear Rate	R^2
4.26	0.67	0.9428
	1.34	0.9715
	2.02	0.9731
	2.70	0.9725

Table 4.9: *Model determination coefficients.*

The determination coefficients show that the model predicts quntitatively good the experimental data. However more tests need to be performed, expecially on the shear rate effect. Indeed in the range studied (from 0.67 to

2.70 s^{-1}) the percolation velocity varies linearly with the shear rate, while observing the model 4.23 is clear that it does not: at high shear rate a plateau trend is expected.

Conclusions

In conclusion it has been shown that granular materials tend naturally to segregate because of different mechanisms. It can be a problem in many industrial process operations (e.g mixing, filling, discharging, conveying), expecially when a high degree of quality is required in product specification. One of these mechanisms is called *percolation*; it occurs when fine particles are able to pass through a bed of coarser ones.

The percolation of bi-dispersed mixtures has been investigated in depth experimentally using a simple shear apparatus, an equipment used to control the system conditions; the experimental measurement method has been sharpen. Beds made of different materials, all characterized by their own shape and sizes, have been tested using the simple shear box. The beds used were made of spherical glass particles and grains made of a mixture of Microcrystalline Cellulose and flour.

From the experiments it has been shown that percolation velocity is strongly dependent on the diameter ratios between the fine and coarse particles; furthermore their behavior can be studied using an exponential law.

The results show that percolation velocity of all particles is also influenced by absolute bed diameter size and shear rate. Specifically the velocity increases linearly with the shear rate and it decreases when the diameter ratio is increased.

On the basis of a previous model presented by *Bertuola et al. (2016)* and the expermental results, a different model is proposed to study the dependency of percolation velocity by the diameter ratio. It has been shown that even if this model fits the experimental data with good results, the exponential model still describes better this behavior.

A comparison between tested granular materials has been shown. Indeed spherical glass particles are very ideal because of their shape and frictional coefficient, while granular materials handled in industries usually presents different characteristcs and behaviors. Hence a deeper analysis is required. Results shows that percolation can be more problematic for the grains, it was not found the precise dependency but it was shown that these properties can slow down the particles percolation time.

Because the particles path is never linear but is always very tortuous, an image analysis has been tried to see if there were any variables which could

influence it. From the results the particles path seems to be totally random; furthermore this analysis was performed during a first moment of this work so it could be that after the measurement method has been sharpen, better results could be found.

It has been seen that there is a new variable, the bed porosity, which was never considered in the percolation relation. Hence a new model has been developed on the basis of theoretical and experimental consideration. In the model only spherical particles are considered. It was shown that the model has a good agreement with the experimental results.

Bibliography

[1] J. Bridgwater (1983) *Mixingand Segregration Mechanisms in Particle Flow.*

[2] M. Rhodes(1998) *Introduction to Particle Technology.*

[3] Richard G. Holdich(2002) *Foundamentals of Particle Technology* Departmment of Chemical Engineernig, Loughborough University, Leicestershire, LE11 3TU, UK.

[4] R.N. Shreve anfd J.A. Brink (1977) *Chemical Process Indutries*, 4th ed. MCGraw-Hill, New-York.

[5] Santomaso Andrea , Canu Paolo , Berloula Davide (2006) *Prediction of Segregation in Funnel and Mass Flow Discharge.*

[6] Williams J.C.(1976) *The Segregation of Particulate Materials.*

[7] Johanson K. , Eckert C. , Ghose D. , Djomlijia M. , Hubert M. (2005) *Quantitative Measurement of Particle segregation Mechanism.*

[8] J. Bridgwater, H.H. Cook and J.A. Drahun (1981) *Strain Induced Percolation.*

[9] J. Bridgwater (2012) *Mixing Powders and Granular Materials by Mechanical Means - A perspective.*

[10] M. Alonso, M. Satoh and K. Miyanami (1991) *Optimum Combination of Size Ratio, Density Ratio and Concentration to Minimize Free Surface Segregation*

[11] A.M. Scott and J. Bridgwater (1975) *Interparticle Percolation:a Foundamental Solid Mixing Mechanism.*

[12] Anjani K. Jha , Virendra M. Puri (2007) *Percolation Segregation of Binary Mixtures under Periodic Movement.*

[13] Anjani K. Jha , Virendra M. Puri (2005) *Innovative Device for Quantification of Percolation and Sieving Segregation Patterns - Single Componenet and Multiple Size Fractions.*

[14] S. P. Duffy and V. M. Puri (2002) *Primaray Segregation Shear Cell for Size-Segregation Analysis of Binary Mixtures.*

[15] N. Khola, C. Wassgren (2015) *Correlations for Shear-Induced Percolation Segregation in Granular Shear Flows.*

[16] M. Rahman(2009) *Foundamental Simluation Studies of Percolation and Segregation of Granular Materials.*

[17] S.C. Yang(2006) *Density Effect on Mixing and Segregation Processes in a Vibrated Binary Granular Mixture.*

[18] J. Bridgwater, W. S Foo, D.J. Stephens(1985) *Particle Mixing and Segregation in Failure Zones- Theory and Experiment.* Powder Technol. 41, 147-158.

[19] A.M. Scott, J. Bridgwater(1976) *Self-diffusion of Spherical Particles in a Simple Shear Celll Apparatus.* Powder Technol. 14, 177-183.

[20] D.J.. Stephens, J. Bridgwater (1978) *The Mixing and Segregation of Cohesionless Particlate Materials: Part I. Failure Zone Formation*, Powder Technol. 21, 17-28.

[21] D.J. Stephens, J. Bridgwater (1978) *The Mixing and Segregation of Cohesionless Particlate Materials: Part II. Microscopic Mechanisms for particles Differing in Size*, Powder Technol. 21, 29-44.

[22] L.B.H. May L.A. Golick, K. Daniels, C. Phillips, M. Shearer (2010) *Shear-driven Size Segregation of Granular Materials: Modeling and Experiment*, Phys. Rev E 81.

[23] F. Bertand,L.-A Leclaire, G. Leveque (2004) *DEM- based Models for the Mixing of Granular Materials.*

[24] A.Rosato F. Prinz (1986) *Monte Carlo Simulation if Particulate Matter Segregation.*

[25] L.R. Lawrance, J.K. Brddow (1968) *Powder Segregation During Die Filling.* Mechanical Engeneering Department, Texas A & M University, College Station Texas 77843 (U.S.A.)

[26] S.B. Savage, C.K.K. Lun (1989) *Particle Size Segregation in Inclined Chute FLow of Dry Cohesionless Granular Solids.* J Fluid Mech 189, 311-355.

[27] H.K. Versteeg and W. Malalasekera (2007) *An Introduction to Computational Fluid Dynamics.* Second edition published 2007, Pearson Education Limited .

[28] R.M. Nedderman (1995) *Statistics and Kinematics of Granular Materials*. Published by Cambridge University Press, Cambridge, UK.

[29] Kunio Shinohara(1979) *Mechanism of Segregation of Differently Shaped Particles in Filling Containers.*

[30] Y. Fan, C.P. Schlick, P.B. Umbanhowar,J.M.Ottino, R.M Lueptow(2014) *Modelling Size Segregation of Granular Materials: The roles of Segregation, Advection and Diffusion* J Fluid Mech 741, 252-279.